Modelling the dynamic behaviour of a PEM fuel cell system

Thesis

E.A. de Mol

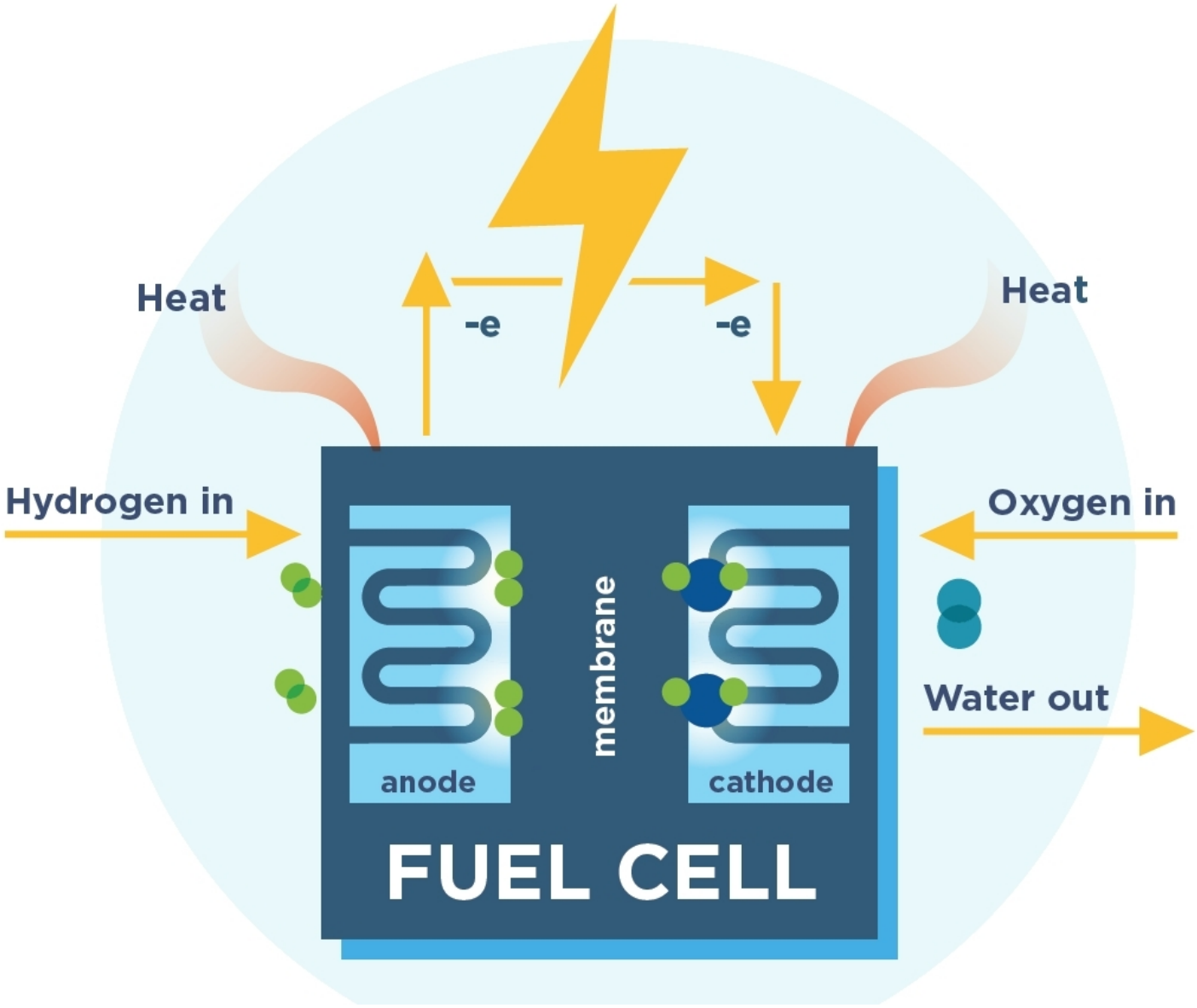

TU Delft Delft University of Technology

Challenge the future

Modelling the dynamic behaviour of a PEM fuel cell system

Thesis

by

E.A. de Mol

to obtain the degree of Master of Science
at the Delft University of Technology,
to be defended on Monday July 24, 2023 at 14:00 AM.

Student number:	4462963	
Project duration:	oct 26, 2020 – July 24, 2023	
Thesis number:	MT.22/23.040.M	
Thesis committee:	Dr. ir. L. van Biert,	TU Delft, supervisor
	Ir. K. Visser,	TU Delft, chairman
	Ir. N. Goselink,	TU Delft

TU Delft

Preface

This is the master thesis ”Modelling the dynamic behaviour of a PEM fuel cell system”. It was written in order to fulfill the graduation requirements of the master Marine Technology at Delft University of Technology.

The subject choice for this thesis fell on fuel cell systems, because of the clean nature of this power generator and because the subject was not discussed in depth within the preceding studies. This subject challenged me to dive further into the working of fuel cells and the modelling environment of Simulink and Matlab. I have learned a lot both academically and on a personal level from the struggles I encountered during the process of implementing the model.

I want to thank my supervisor, Dr. ir. Lindert van Biert, for the continued guidance during the writing of this thesis. Furthermore, I want to thank my family and friends, with special mention to my sister-in-law, for the support given in order to finish the thesis.

E.A. de Mol
Dordrecht, April 2023

Contents

1 Introduction

Following the IMO 2020 regulation, ships need to reduce sulphur emissions everywhere in the world. This is only one example of more strict regulations currently being implemented to ensure a global reduction of greenhouse gases. The change towards a cleaner shipping industry also requires research into alternatives for the current use of combustion engines. Options for a cleaner power source would be using cleaner fuels for the combustion engine or scrubbing the exhaust gases to lower the harmful emissions. However, another option would be to find an alternative for the combustion engine itself, namely a fuel cell.

1.1. Potential of fuel cells

Fuel cells are currently gaining interest with the maritime branch and within other industries as well. They are however not a brand new invention since the first fuel cell was already created in 1839, but they were not applied within the industry until after the 1960's. A fuel cell combines hydrogen and oxygen to water and collects the electricity that is released during the electrochemical reaction. The main advantage of a fuel cell lies in the fact that water is the only emission, contrary to an air operated hydrogen internal combustion engine which has NOx emissions as well and thus a very clean energy conversion. The absence of harmful emissions is not the only advantage of a fuel cell which makes a fuel cell an interesting power source for many applications. Other advantages are the expected high efficiency, the simplicity in the design promising a low cost, the small weight and size of the cell, and the absence of moving parts promising less maintenance for the fuel cell. Some of these advantages are especially important in some marine applications. For example, the fact that the fuel cell has no moving parts also ensures less noise and vibrations which is highly desirable on board of cruise ships where passenger comfort is the main goal. Some of the challenges with implementing fuel cells on ships are due to the large power demand of ships and the difficulties in storing the necessary amounts of hydrogen on board. Oceangoing vessels are therefore not part of the target group for implementing fuel cells. However, inland vessels including ferries, inland cruise ships, and harbour patrol ships are a realistic possibility to implement fuel cells in. The challenge with using fuel cells in ships right now is that the reactions of the fuel cell system to different scenarios are not well known.

1.2. Problem introduction

In order to apply fuel cells within ships it is important to know how the fuel cell system reacts to changes in the requested load. How long does it take for the system to come to a full stop? How long before the system is running at full power? Is this fast enough for ships to operate as expected? And how does the duty cycle of the ship affect the consumption of the hydrogen? There are a lot of steady-state and dynamic models created in to describe the behaviour of a fuel cell or stack under load changes. However, the effect of the load changes on the auxiliary systems needed to keep the fuel cell operating at the desired condition is usually not taken into account. It is important to include the balance of plant of the fuel cell when modelling the behaviour since the auxiliary systems influence the fuel cell. A model describing the complete system in order to research the required inputs into the system and the outputs

has not been applied within the field of marine technology yet. Papers researching the balance of plant of a fuel cell system do not fully describe the creation of the model and are therefore not able to be completely reproduced such as the papers of Rabbani and Rokni (2013) and Yang et al. (2019).

1.3. Research Objectives

The research objective of this thesis is to simulate the dynamic behaviour of a proton exchange membrane (PEM) fuel cell system. The model will encompass the fuel cell and its balance of plant. It will focus on simulating the reactions of the cell and its systems with regards to changes in the requested load. In order to fulfil the thesis objective, several subquestions are formulated:

- What models currently exist to simulate a fuel cell?
- How to model the stacking of multiple fuel cells?
- What auxiliary systems are necessary for the operating of a PEM fuel cell?
- Which parameters affect fuel cell operation the most?
- How do the auxiliary components affect the transient response?
- How does a maritime duty cycle affect fuel consumption and stack operation?

1.4. Outline

The approach to this model will be first to study existing literature on the subject as will be given in the following chapters. Firstly, the functioning of a fuel cell in general will be researched. Then the models previously created to simulate the fuel cell will studied in order to find suitable models to implement in a complete system model. These models are described in Chapter 2.
In this chapter the auxiliary systems needed to operate the fuel cell will also be discussed. After the first three subquestions are sufficiently answered in the literature study, the modelling of the system will start. Based on the existing models a dynamic model for the fuel cell will be created with Matlab and Simulink. The implementation of this model is discussed in Chapter 3. In Chapter 4, the implemented model will be verified and validated with respect to the existing models found in the literature study if possible. The model will be used to simulate the duty cycles of a representative ship and their effect on the fuel cell system. This will give more information on the response time of the system to load changes and the expected fuel consumption with different scenarios. In the last chapter the conclusion will be given followed by recommendation to improve or expand this research.

2

PEM fuel cell

In this chapter the theoretical model of a fuel cell stack will be discussed. The chapter starts with the theory behind the fuel cell and the stacking of the fuel cells. Thereafter this chapter will discuss the approaches used to model the fuel cell stack currently used in literature. The approach is divided in three main parts being the electrochemical balance, the mass flow model, and the heat balance.

2.1. Working principle of the fuel cell

The fuel cell converts the fuel into electricity through an electrochemical reaction. Energy losses occur during this reaction in the form of heat. The proton exchange membrane fuel cell (PEMFC) has a polymer electrolyte membrane separating the two electrodes and the gas diffusion layers which allow the hydrogen and oxygen reactions to happen at the anode and cathode. Hydrogen is fed at the anode in gaseous state where the molecules are split into electrons and ions. The negative anode allows the electrons to flow through an external load and to the positive electrode. The hydrogen ions simultaneously permeate through the membrane whereafter they combine with the hydrogen electrons and the oxygen molecules at the cathode side producing water. The PEMFC could also work with fuels containing hydrogen and with air instead of pure oxygen. This would then give different exhaust products next to water. Focusing on pure hydrogen-fuelled PEMFC, the working chemical reaction 2.3 is as follows, with the anode half-reaction 2.1, the cathode half-reaction 2.2 shown:

$$H_2 \leftrightarrow 2e^- + 2H^+ \tag{2.1}$$

$$\frac{1}{2}O_2 + 2e^- + 2H^+ \leftrightarrow H_2O \tag{2.2}$$

$$H_2 + \frac{1}{2}O_2 \leftrightarrow H_2O + heat + electrical\ energy \tag{2.3}$$

While the working principle of a fuel cell seems simple, it needs to operate within specific conditions to work effectively. In order to maintain these conditions a set of auxiliary components is necessary to complete the fuel cell system. The auxiliary components will be discussed further at the end of this chapter.

2.2. Stacking of the fuel cell

A single fuel cell cannot meet the power demand of modern day appliances, vehicles, and in this case ships. To meet this power demand, the fuel cells are connected in series to make a stack. The stack size is dependent on the size of the cells and the amount of cells within the stack and can be chosen by the producer. By stacking the fuel cells larger voltage potentials and thus higher powers can be generated. Within the stack each cell has its own oxygen and hydrogen feed. However, each cell also generates heat during the chemical reaction thus raising the temperature within the cell and the neighbouring cells. This means that the cells are not operating under equal conditions.

Models looking at cell specific behaviour are too computational consuming in order to use for a full system analysis. Literature studying the balance of plant therefore assume the fuel cells in the stack to be equal when simulating dynamic fuel cell behaviour. This assumption is applied in this model as well.

2.3. Modelling approaches

Modelling within literature is done in general with respect to three aspects; the electrochemical balance, the mass flow balance, and the energy balance.

2.3.1. Electrochemical balance

The electrochemical balance is usually modelled steady-state, because the order of magnitude in timescale is significantly smaller than the order of magnitude in timescale of the mass flows and the energy flows (Del Real et al., 2007). Thus, the changes modelled within the electrochemical model will appear instantaneous on the time scale of a dynamic model which simulates the behaviour of the mass and heat transfer.

The electrochemical model gives the voltage output for the different current levels. The model is based upon the theoretical fuel cell potential with several losses taken into account. In order to determine the theoretical cell potential, first the Gibbs free energy is calculated. The Gibbs free energy is the thermodynamic potential giving the maximum available work from the conversion of chemical energy into electrical energy. The Gibbs free energy is given in equation 2.4. The specific Gibbs free energy ($\overline{g}_f^0$) is dependent on the temperature, pressure, and gas phase and will be calculated at standard conditions.

$$\Delta\overline{g}_f^0 = (\overline{g}_f^0)_{H_2O} - (\overline{g}_f^0)_{H_2} - \frac{1}{2}(\overline{g}_f^0)_{O_2} \tag{2.4}$$

In an ideal reversible fuel cell, the Gibbs free energy would be the same as the maximum electrical work (W_{el}). With the equation for electrical work, equation 2.5 can be derived.

$$W_{el} = \Delta G^0 = -n * F * E^0 \tag{2.5}$$

Rewriting this equation will give a definition for the ideal fuel cell potential E^0 (2.6), with F being Faraday's constant, n the amount of electrons, which for hydrogen oxidation in a fuel cell reaction is 2.

$$E^0 = \frac{-\Delta G^0}{2 * F} \tag{2.6}$$

A PEMFC has an operating temperature of around 80 degrees Celsius and, therefore, the previous equation will have to be adapted since it only is valid for standard temperature and pressure. The adaptation in order to account for the chemical activities of the reactants and products is given in the Nernst equation. The more correct theoretical fuel cell potential is then given by equation 2.7 below.

$$E = E^0 + \frac{R * T}{2 * F} \ln\left(\frac{a_{H_2} * a_{O_2}^{\frac{1}{2}}}{a_{H_2O}}\right) \tag{2.7}$$

Within the Nernst equation, R is the universal gas constant and T the temperature in the fuel cell. Furthermore, a is the activity as defined as below (2.8), with P_i being the partial pressure of the gases and P_0 the standard pressure:

$$a = \frac{P_i}{P_0} \tag{2.8}$$

Assuming the gases to behave like ideal gases and the activity of water equal to 1, the Nernst equation can be simplified. The theoretical cell voltage is now dependent on the partial pressures of hydrogen and oxygen, and on the stack temperature.
The actual cell voltage output of a fuel cell will be lower due to losses. Firstly, the activation overpotential is the loss due to overcoming the activation energy of the cell reactions. The activation loss on both

the anode and cathode side can be calculated using the Tafel equation when assuming equal transfer coefficients in both electrodes and the activation losses to be larger then zero. The Tafel equation (2.9) the becomes:

$$V_{act} = V_{act,c} + V_{act,a} = \frac{R * T}{\alpha_c * F} \ln\left(\frac{i + i_{loss}}{i_{0,c}}\right) + \frac{R * T}{\alpha_a * F} \ln\left(\frac{i + i_{loss}}{i_{0,a}}\right) \tag{2.9}$$

The subscript a refers to the anode and c to the cathode side. The transfer coefficients α (eq. 2.10 and 2.11) and the value for the exchange current density i_0 (eq. 2.12 and 2.13)can be evaluated using the method used by Rabbani and Rokni (2013). The variable $n_{e,a}$ and $n_{e,c}$ are the number of electrons for the anode and the cathode in this reaction, respectively 4 and 1.

$$\alpha_a = \beta * n_{e,a} \tag{2.10}$$

$$\alpha_c = (1 - \beta) * n_{e,c} \tag{2.11}$$

The exchange current density function has as the inputs the variables stack temperature, T_{stack}, and the theoretical cell potential, E^0. The parameters in the function are the following: a symmetry factor β set to 0.5, the number of electrons n, Faraday's constant F, reaction rate coefficient k, and the gas constant R. The exchange current density is then calculated as shown in equations 2.12 and 2.13 for the anode and cathode respectively:

$$i_{0,a} = n * F * k_a * e^{(1-\beta)*n*F*\frac{E_0}{R*T_{stack}}} \tag{2.12}$$

$$i_{0,c} = n * F * k_c * e^{(-\beta)*n*F*\frac{E_0}{R*T_{stack}}} \tag{2.13}$$

The losses due to fuel crossover and internal current generation, i_{loss} were assumed to be constant at $0.002 A/cm^2$ as reasoned by Rabbani and Rokni (2013).
Secondly, Ohmic overpotential is due to resistance in the ionic flow and in the electron flow and due to contact resistance at the terminals of the bipolar plates. The Ohmic overpotential follows the Ohmic law. The Ohmic losses are calculated according to the following formula (2.14):

$$V_{Ohmic} = (r_{el} + r_{ion}) * i \tag{2.14}$$

The electronic resistance (r_{el}) is very small compared to the ionic resistance (r_{ion}) and is therefore often left out of the summation of the Ohmic resistance. The ionic resistance can be calculated in two ways. Either with the formula created for a Nafion 117 membrane as used by Jia et al. (2009) and Rabbani and Rokni (2013) or with the other method proposed in literature and given by Rabbani and Rokni (2013) which is a simpler correlation based upon the membrane thickness and the membrane activity. The equation specific for the Nafion117 membrane also takes the current into account when calculating the ionic resistance. This is preferable since the model will be transient and the current will be expected to change and thus the ionic resistance is expected to change as well.

Thirdly, the concentration overpotential is caused by smaller concentrations of the reactants at the interface of the electrode and membrane. These losses occur mainly at high currents and are very small at lower currents. This is the reason that it sometimes is neglected in modelling, as done by Xue et al. (2004). Another method is proposed by Rabbani and Rokni (2013) where the current densities are limited based upon the stoichiometric ratio of the reactants. Due to the losses only occurring at high currents and high currents being negative for a long stack life and higher efficiencies, the losses will within standard operation not occur. The concentration losses can therefore be neglected in the model.

2.3.2. Flow modelling

To model the flow of mass in the fuel cell, a molar balance is set up for the anode and cathode outlet following the same method Rabbani and Rokni (2013) used. The main assumptions used within the stack are that there is no phase change. This means that all species are in gas phase and all gases

follow the ideal gas law. The mass and thus molar flows are modelled assuming steady-state flow. The molar rate is predicted using Faraday's law 2.15 for the reactants at a specific current.

$$\dot{n}_{H_2} = \frac{I}{n * F} * S_{H_2} \tag{2.15}$$

Herein S_{H_2} is the stoichiometric ratio for hydrogen at a particular current. The molar balance at the anode is given by the following equations:

$$\dot{N}_{H_2,out} = \dot{N}_{H_2,in} - \frac{i + i_{loss}}{2F} * A_{cell} * N_{cells} \tag{2.16}$$

$$\dot{N}_{H_2O,a,out} = \dot{N}_{H_2O,a,in} + (J_{H_2O} * A_{cell} * N_{cells}) \tag{2.17}$$

$$\dot{N}_{N_2,a,out} = \dot{N}_{N_2,a,in} + (J_{N_2} * A_{cell} * N_{cells}) \tag{2.18}$$

With J_{H_2O} and J_{N_2} being the water and nitrogen flux respectively. The nitrogen flux is dependent on the partial pressures of the anode and the cathode of the fuel cell. The water flux is the difference between the electro-osmotic drag and the back diffusion. These fluxes can be calculated similarly to Rabbani and Rokni (2013) and will be further explained in section 3.5.2. The parameters A_{cell} and N_{cells} are the cell area and the number of cells in the stack.
The molar balance at the cathode outlet is set up the same as the anode side and the corresponding equations are shown below:

$$\dot{N}_{O_2,out} = \dot{N}_{O_2,in} - \frac{1}{2}\left(\frac{i + i_{loss}}{2F}\right) * A_{cell} * N_{cells} \tag{2.19}$$

$$\dot{N}_{H_2,c,out} = \dot{N}_{H_2,c,in} + \frac{i + i_{loss}}{2F} * A_{cell} * N_{cells} - (J_{H_2O} * A_{cell} * N_{cells}) \tag{2.20}$$

$$\dot{N}_{N_2,c,out} = \dot{N}_{N_2,c,in} - (J_{N_2} * A_{cell} * N_{cells}) \tag{2.21}$$

$$\dot{N}_{CO_2,out} = \dot{N}_{CO_2,in} \tag{2.22}$$

$$\dot{N}_{Ar,out} = \dot{N}_{Ar,in} \tag{2.23}$$

2.3.3. Energy balance

The heat generation within the fuel cell is determined with the energy balance under the same assumptions as the mass model. This method is, for example, used by Amphlett et al. (1996), Rabbani and Rokni (2013), and Yu et al. (2005). The transient model gives the temperature change with respect to time as shown in equation 2.24.

$$\frac{dT_{stack}}{dt} = \frac{q_{theo} - q_{elec} - q_{sens} - q_{latent} - q_{loss}}{m_{stack} * C_{p,stack}} \tag{2.24}$$

Herein m_{stack} is the mass of the fuel cell stack and $C_{p,stack}$ the average specific heat of the stack. The theoretical energy q_{theo} is given by multiplying the molar flow rate of consumed hydrogen with the enthalpy of combustion,$\Delta H_{reaction}$, as shown in equation 2.25. The enthalpy of combustion for hydrogen is determined in experiments and is equal to 286000 J/mol.

$$q_{theo} = \dot{N}_{H_2,cons} * \Delta H_{reaction} \tag{2.25}$$

The electrical energy (q_{elec}) is calculated with the voltage of the cell (V_{cell}), the number of cells (N_{cells}), and the output current i (2.26).

$$q_{elec} = N_{cells} * V_{cell} * i \tag{2.26}$$

The sensible heat is the sum of the sensible heat through the anode, the cathode, and the water coolant stream. These sensible heats are calculated by considering all the possible species going in (subscript $_{in}$) and out (subscript $_{out}$) the anode or cathode respectively. The sensible heat for the anode can be summarised in the following formula (2.27) with i denoting the species:

$$q_{sens,a} = \sum_i \dot{N}_{i,out} * C_{p,i} * (T_{out} - T_0) - \dot{N}_{i,in} * C_{p,i} * (T_{in} - T_0) \tag{2.27}$$

Herein, the $\dot{N}_i$ is the molar flow of the species i, $C_{p,i}$ is the specific heat capacity of the species i, and T_{in}, T_{out}, and T_0 are the temperatures going in and out of the fuel cell and the reference or room temperature respectively. The sensible heat in the cathode is calculated in a similar manner with the species occurring at the cathode. The sensible heat in the water coolant stream follows the same principle with the species being the liquid water and the temperatures of the water coolant in and out of the cell.
The latent heat is denoted by Yu et al. (2005) as the sum of the latent heat of the anode and the cathode. The latent heat of the anode is calculated with equation 2.28.

$$q_{latent,a} = (\dot{N}_{w,g,a,out} - \dot{N}_{w,g,a,in} + \dot{N}_{trans}) * H_{vaporisation,a} \tag{2.28}$$

The $\dot{N}_{trans}$ is the molar flow rate of the water transfer across the membrane which is assumed to be in vapour form. $\dot{N}_{w,g,a,out}$ is the molar flow of water in gaseous state going out the anode and $\dot{N}_{w,g,a,in}$ is the molar flow into the anode. $H_{vaporisation}$ is calculated with formula 2.29 in which the temperature is in Kelvin.

$$H_{vaporisation} = 45070 - 41.9 * T + 3.448 * 10^{-3} * T^2 + 2.54 * 10^{-6} * T^3 - 8.98 * 10^{-10} * T^4 \tag{2.29}$$

The cathode latent heat is calculated the same as the latent heat at the anode side since all water is assumed to be steam and no phase change is present within the fuel cell stack. Yu et al. (2005) does not make the assumption of all species being in gas phase and therefore differs in the approach for the calculation of the cathode latent heat. Because the assumption is made here, the latent heat of the cathode is equal to:

$$q_{latent,c} = (\dot{N}_{w,g,c,out} - \dot{N}_{trans} - \dot{N}_{w,g,c,in}) * H_{vaporisation,c} \tag{2.30}$$

The last heat term in equation 2.24 to be determined is the heat loss q_{loss}. The heat loss will be transient and is calculated using equation 2.31 for the natural convection and radiation to the surroundings as is done by Musio et al. (2011).

$$q_{loss} = \frac{T_{stack} - T_{amb}}{R_{th}} \tag{2.31}$$

The thermal resistance R_{th} will be assumed constant and is determined by calculating the heat loss in steady-state operation.

2.3.4. Spatial dimension of the model

Lumped-parameter models are the preferred choice to model fuel cells at system level. 2D and 3D spatial models do exist, but these are specifically for details within a part of a fuel cell, such as the research done by Tadbir et al. (2012) and C.-Y. Wang (2004), and they are not as useful for looking at the entire balance of plant. The aim for this research will thus be on a lumped-parameter model as proposed by Sharifi Asl et al. (2010) and Xue et al. (2004).

2.4. Auxiliary systems to the PEM fuel cell

In order to maintain the correct operating conditions in the fuel cell, several systems are used which make up the balance of plant. These systems are a heat exchanger to regulate the temperature in the fuel cell, an air compressor to regulate the pressure of the air flow entering the fuel cell, an air cooler and humidifier to regulate to inflow temperature and humidity, and finally a valve to regulate the inflow of hydrogen. These systems are also shown in figure 2.1.

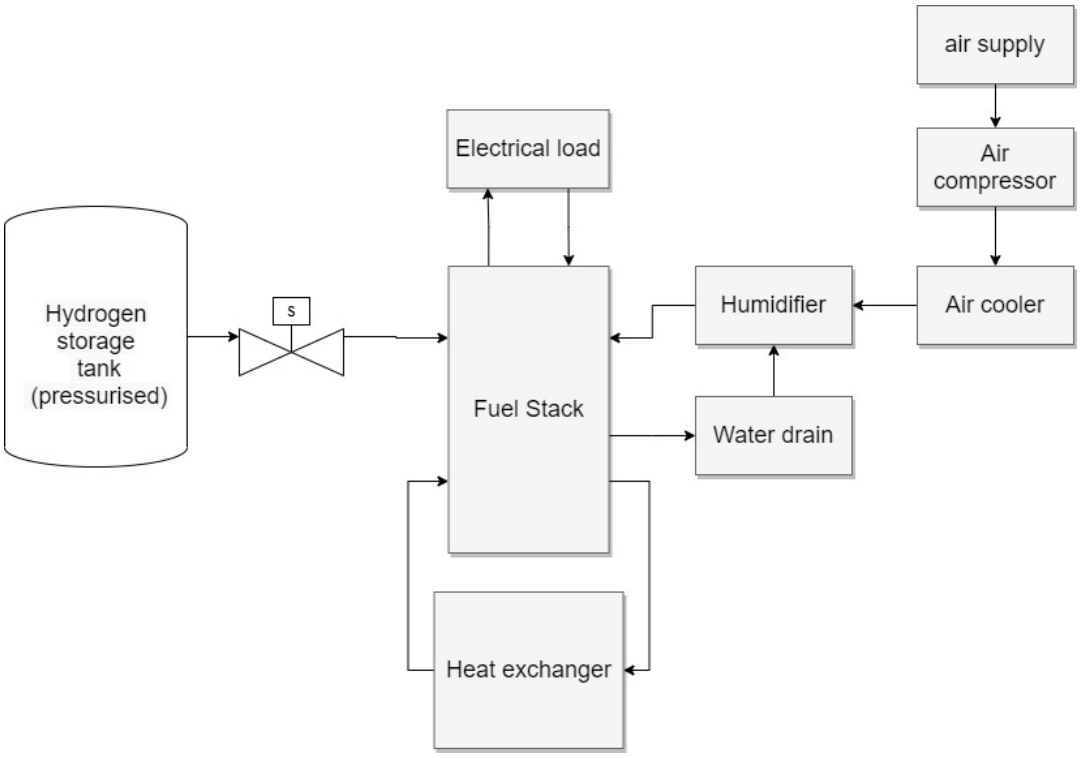

Figure 2.1: PEM fuel cell including the balance of plant

3

Implementation of the model

The model is implemented in Simulink. The Simulink model is run via a Matlab script which also loads the parameters into Simulink and post-processes the Simulink data. The parameter script (Appendix B) and the Simulink implementation of the submodels (Appendix A) are shown in the appendices.

While implementing the model, the choice was made to focus on the implementation of the fuel cell stack itself before starting on the implementation of the balance of plant components. The implementation of the fuel cell stack gave rise to instabilities in the model, which need to be solved first in order to expand the model. This is the reason why the implementation of the balance of plant is removed from the scope of this thesis.

3.1. List of assumptions

The model is created under the following assumptions:

- All species in gaseous form in the system follow ideal gas law
- All species enter the system in gaseous form
- Carbon dioxide and argon are considered non-reactive species in the air flow
- Flows are laminar
- Pressure changes are instant
- Thermal resistance is assumed constant
- Concentration losses can be neglected
- Only the ionic resistance is considered in the ohmic resistance
- The changes in the electrochemical balance are instantaneous
- All cells in the fuel cell stack are the same
- Flow changes due to pumps are modelled instantaneous

3.2. Structure of the model

The model is structured in a main model with four submodels. These submodels are interconnected by several variables having dependencies on each other. The main model has the stack temperature, the current, the molar flows of hydrogen, air, nitrogen, and the molar flow of the coolant as the input variables. Furthermore, the temperatures, pressures and relative humidities at the inlets of both the anode and cathode are necessary to calculate the power output of the stack. The other outputs of the main model are the updated values of the stack temperature and the relative humidities which can then be used for the next iteration.

The four submodels match the three models described earlier in the previous chapter and include an additional submodel for the calculations regarding the pressures and partial pressures in the fuel cell. Since the electrochemical balance, molar flow, pressures and partial pressures, and energy balance submodel blocks all have input variables which are dependant on the outputs of at least one of the other submodels, first the interdependencies will be explained. The schematic overview of the four submodels in the fuel cell stack model with the interdependencies are shown in figure 3.1. The first submodel is the electrochemical balance submodel. This submodel calculates the power output of a single cell. The second submodel which will be discussed is the molar flow model wherein the flows will be calculated. These flows are also necessary to determine the partial pressures and the losses in the energy balance. The third submodel is the pressures and partial pressures submodel. This submodel is created since the molar flow model and the electrochemical balance model both require the partial pressures as an input. The fourth submodel is called the energy balance and calculates the change in temperature.

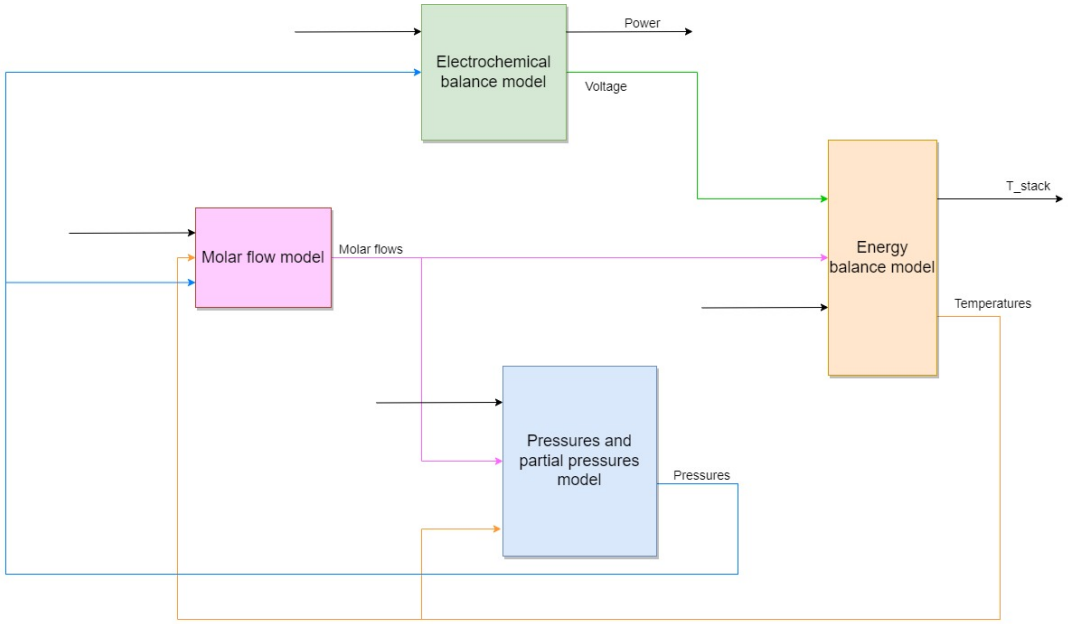

Figure 3.1: Schematic overview of the four submodels in the fuel stack model with variable interdependency shown. The black lines represent all the variables that are not causing algebraic loops.

3.3. Dependant input variables

The input variables, which are simultaneously the output variables from a different submodel, create algebraic loops in the model which are sometimes numerically impossible to solve. The dependant variables and how they are connected to the different submodels are addressed here.

Firstly, the electrochemical model uses the partial pressures of hydrogen and oxygen during its calculations. These two variables are calculated in the pressures model, but do not create a loop and thus do not need additional measures to solve.

Secondly, the molar flow model contains the partial pressures of nitrogen, the pressures at the outlets, and the temperatures at the outlets at both the anode and cathode side of the fuel cell that are dependant on the outputs of other submodels. The pressure related input variables are calculated in the pressures submodel, which in turn depends on the outputs of the electrochemical model. This is resolved using a memory block for the partial pressures of nitrogen so the value of the previous iteration is used during the calculations to prevent the need to solve additional algebraic loops. The pressures at the outlets of the anode and cathode are directly connected to the input ports of the electrochemical model, since the pressures barely change and the solver is thus able to handle the resulting algebraic

loops. The temperature related inputs are calculated in the energy balance model which is dependent directly on the outputs of the electrochemical model as well. The choice is made to let the model solve the algebraic loop each iteration, because the model is able to do so without issues.

Thirdly, the pressures model is the most interconnected of the submodels since the input variables include all the outputs of the molar flow model and the temperatures at the outlets from the energy balance model. The loops with the molar flow model are resolved with the memory blocks on the outputs as explained above with regards to the inputs of the molar flow model. The algebraic loop with the energy balance model exists due to the use of temperatures that are calculated in the energy balance model. This loop was kept in the model and is solved by the solver each iteration.

Lastly, the inputs of the energy balance model are either main model inputs from the hypothetical balance of plant or from the electrochemical model or molar flow model. The dependency of those models on the outputs of the heat model resides in the dependence on the stack temperatures. However, the stack temperature being calculated in the energy balance model is not used until the next iteration and thus does not cause problems during solving. The temperatures at the outlets of the anode and cathode are used directly by the molar flow model and include an algebraic loop during solving.

3.4. Electrochemical model

The electrochemical model is a model for a single cell in the stack and will afterwards be multiplied for the amount of cells in the stack.

3.4.1. The input and output variables

The submodel has the following inputs: stack temperature, molar flow of hydrogen per cell, current density, partial pressures of hydrogen and oxygen, and water content of the membrane (fig. 3.2). The water content of the membrane is calculated as shown in equation 3.3.

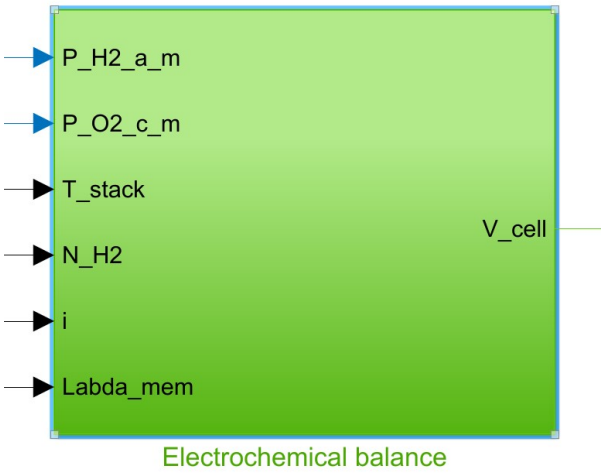

Figure 3.2: Overview of the input and output variables of the electrochemical submodel

Inside the submodel the calculations as described in the previous chapter are performed. The detailed submodel is shown in Appendix A.1.

3.4.2. Gibbs free energy

First the temperature dependant Gibbs free energy for the oxygen, hydrogen, and water are calculated. The temperature dependant Gibbs free energy is calculated as explained by Moran et al., 2012:

$$g_f = g_f^0 + h_f - (T_{stack} * s_f - T_{ref} * s_{f,ref}) \tag{3.1}$$

The implementation of the Gibbs free energy and the theoretical cell potential is shown in figure 3.3.

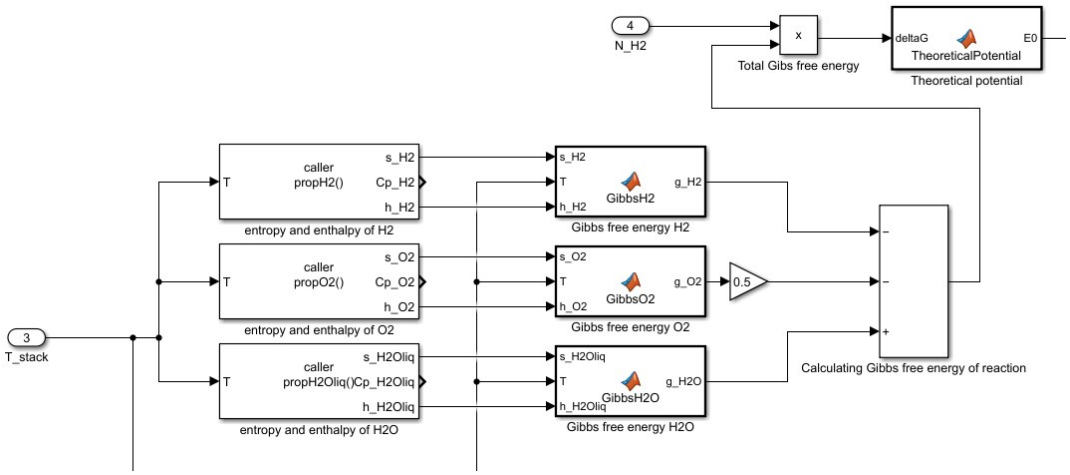

Figure 3.3: The implementation of the Gibbs free energy calculation

Herein the reference temperature is set at the room temperature for this case and the reference entropy at the entropy at room temperature. The values for entropy and enthalpy at stack temperature are derived using the Steam tables script (Holmgren, 2023) which is called upon from the Simulink model with a caller function as shown in figure 3.3. Thereafter, the Gibbs free energy is calculated as explained in chapter 2, which is implemented as a simple function for H_2, O_2, and H_2O separately and thereafter added to each other forming the total Gibbs free energy. This is described in equation 2.4. Before the next step, implementing the equation for the theoretical fuel cell potential (2.6), the Gibbs free energy is multiplied with the hydrogen molar flow to give the actual Gibbs free energy produced in the cell per second. Lastly, the theoretical cell potential is calculated exactly as described in chapter 2.

This theoretical cell potential is then used for two different calculations. Firstly, the exchange current densities needed to calculate the activation losses are determined using the cell potential. Secondly, the theoretical cell potential will have additional terms added in the Nernst equation 2.7.

3.4.3. Theoretical fuel cell potential

Starting with the Nernst equation for theoretical fuel cell potential, the other inputs for this equation are the stack temperature and the pressures and saturated pressures of both hydrogen and oxygen. Any other parameters used are given in the parameter script as added in Appendix B. The potential is calculated as described in chapter 2. For completeness, the calculation of the activities of hydrogen and oxygen is included within the same function. The saturated pressures used for this function are determined in a separate function beforehand with the Steam tables script and are based on the average temperatures of the anode and cathode as can be seen in figure 3.4.

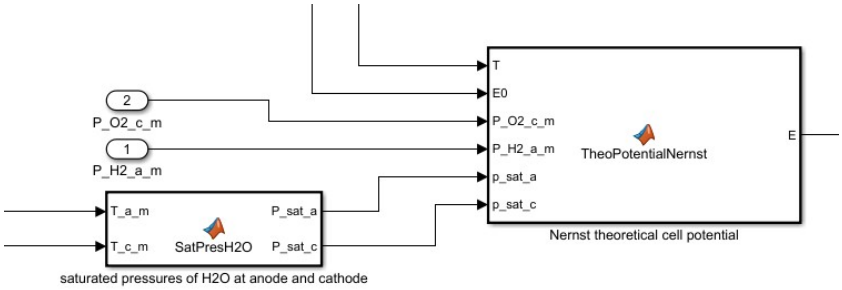

Figure 3.4: The implementation of the Nernst theoretical fuel cell potential calculation

3.4.4. Activation losses

The first of the losses which are calculated are the activation losses. The activation losses are dependant on the exchange current density as explained in section 2.3. The functions 2.12 and 2.13 for the exchange current density are implemented as MatLab functions as shown in figure 3.5. The variables stack temperature (T_{stack}) and theoretical cell voltage (E_0) are the inputs shown in the figure. For simplicity the stack temperature is denoted in the figure using only a T instead of T_{stack} The parameters of the function are all constants and predefined in the parameter script and thus available in the workspace. This means that the inputs for the function can be called upon directly from the workspace.

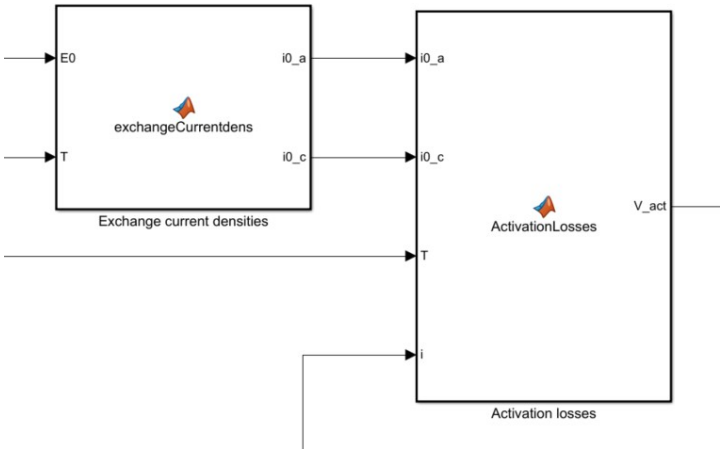

Figure 3.5: The implementation of the current exchange density and activation losses

With the exchange current densities for the anode and cathode determined, the activation losses can be calculated. Besides the exchange current densities (i_0), the other variable inputs of the activation losses function are the stack temperature (T_{stack}) and the current density (i) (see figure 3.5). The losses are calculated according to equation 2.9 in this function. Thereafter, the activation losses are subtracted from the Nernst theoretical cell potential.

3.4.5. Ohmic losses

The second losses which are subtracted from the cell potential are the Ohmic losses. The Ohmic losses are the determined by multiplying the resistance with the current density. The resistance has two components, however only the ionic resistance is modelled since the electronic resistance is negligible as explained in the chapter 2. The ionic resistance is calculated using the formula for the Nafion117

membrane (eq. 3.2).

$$R_{ion} = \frac{C_1 * (1 + 0.03 * i + 0.062 * \frac{T_{stack}}{303}^2 * i^{2.5})}{(\lambda_{mem} - 0.634 - 3 * i) * e^{C_2 * \frac{T-303}{T_{stack}}}} * t_{mem} \tag{3.2}$$

C_1 and C_2 are constant and are respectively 180 and 16.4 as obtained from Rabbani and Rokni (2013). The t_{mem} is the thickness of the membrane and is a set parameter.

When the losses have been subtracted, the output of the electrochemical submodel has been calculated and is equal to the voltage for a single cell. The implementation of the Ohmic losses followed by the subtraction of the Ohmic losses and the activation losses from the Nernst theoretical fuel cell potential are shown in figure 3.6.

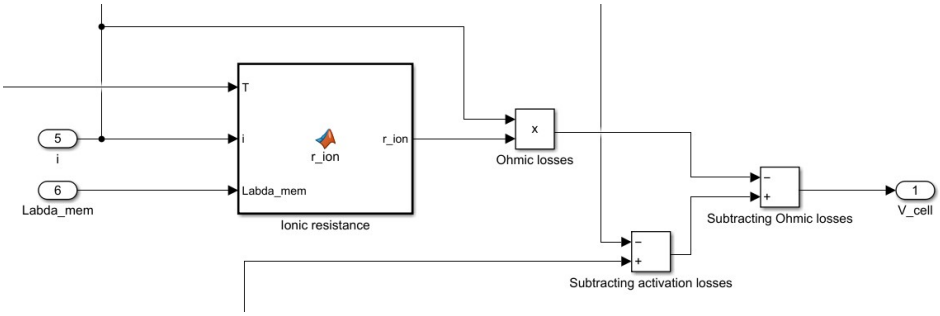

Figure 3.6: The implementation of the Ohmic losses calculation and the substraction of losses from the theoretical potential

3.5. Molar flow model

The second submodel which will be discussed is the molar flow model. The molar flows are calculated directly for the entire stack and not for the individual cells within the stack.

3.5.1. The input and output variables

The variable inputs which are needed for the calculations regarding the molar flows are shown in figure 3.7. These are summarised as the molar flows of air and water, the temperatures throughout the stack, the pressures at the entrances and exits of the stack, the partial pressures of nitrogen at both the anode and cathode sides, the relative humidities for both the anode and cathode, and finally the current density and membrane water content.

The output variables are the molar flows of each individual species for the anode and cathode separately. The molar flow of water is specified to be in either the liquid state or the gas state when exiting the stack. The single output variable that is not a molar flow entering or exiting the stack, is the amount of water that is transported to from the anode to the cathode (this variable is named $\dot{N}_{H_2O,trans}$).

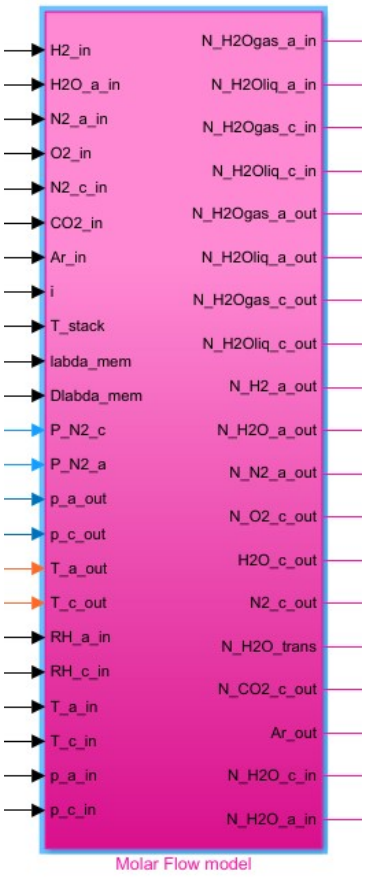

Figure 3.7: Overview of the input and output variables of the Molar Flow submodel

The membrane water content is calculated outside of the submodel. The input variables average membrane water content, λ_{mem}, and the difference in membrane water content between the anode side and the cathode side, $\Delta\lambda_{mem}$, are both dependent on the membrane water content of the anode and cathode side, which are calculated using equation 3.3. The formula used for the membrane water content is dependent on the water activity (a_w) being smaller or greater than 1. Because of this assumption made for this model, the water activity is equal to the relative humidity. The relative humidity is calculated as described in section 3.8.

$$\lambda = \begin{cases} 0.043 + 17.18 * a_w - 39.85 * a_w^2 + 36 * a_w^3 & \text{if } a_w\text{<1} \\ 14 + 1.4 * (a_w - 1) & \text{if } a_w\text{>1} \end{cases} \tag{3.3}$$

Appendix A.2 contains an overview of the inside of the molar flow submodel.

3.5.2. Water and nitrogen transport

Within the submodel block, the first calculations include the water and nitrogen flux. These fluxes are necessary to determine the water and nitrogen transport from the cathode to the anode.

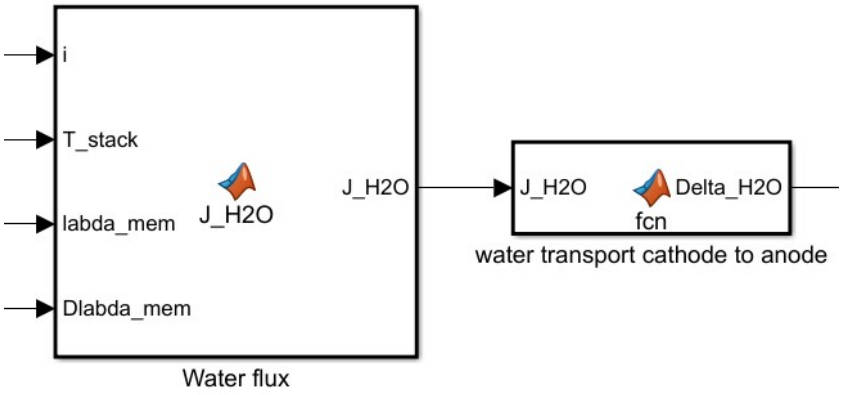

Figure 3.8: The implementation of the water flux calculation

The water flux (J_{H_2O}) calculation is as described by Rabbani and Rokni (2013) and shown below in equation 3.4.

$$J_{H_2O} = \frac{\rho_{mem,dry}}{M_{mem}} * D_w * \frac{\Delta\lambda_{mem}}{t_{mem}} - \frac{2 * n_{drag} * i}{n_{H_2} * F} \tag{3.4}$$

The parameters density of dry membrane ($\rho_{mem,dry}$), membrane thickness (t_{mem}), molecular weight of membrane (M_{mem}), and the number of electrons for H_2 (n_{H_2}) are given as constants in the parameter script and are accessed directly from the workspace. The variables current density (i), stack temperature (T_{stack}), membrane water content (λ_{mem}), and difference in membrane water content of the anode and cathode ($\Delta\lambda_{mem}$) are changing inputs which are also shown in figure 3.8 and are used to either calculate the water flux or another variable necessary to calculate the water flux. The calculation steps to determine electro-osmotic drag (n_{drag}), the membrane water content coefficient (D_λ), and the water diffusion coefficient (D_w) are shown below:

$$n_{drag} = n_{drag_{sat}} * \frac{\lambda_{mem}}{22} \tag{3.5}$$

$$D_\lambda = 10^{-6} * (2.563 - 0.33 * \lambda_{mem} + 0.0264 * \lambda_{mem}^2 - 0.000617 * \lambda_{mem}^3) \tag{3.6}$$

$$D_w = D_\lambda * e^{2416*(\frac{1}{303} - \frac{1}{T_{stack}})} \tag{3.7}$$

The above calculated flux is per area and is thus multiplied by the area of a single cell and the total number of cells in the stack. The total transported water from the cathode to the anode is then used to determine the amount of water in the anode and cathode after the reaction. For the variable $\dot{N}_{H_2O,trans}$, the transported water is multiplied by negative one due to a different definition in the positive direction of the flow used in the energy balance.

The nitrogen flux (J_{N_2}) is calculated as follows:

$$J_{N_2} = K_{N_2} * \frac{P_{N_2,c} - P_{N_2,a}}{t_{mem}} \tag{3.8}$$

The permeation K_{N_2} is calculated beforehand in the same block with the formulae and parameters:

$$f_v = \lambda_{mem} * \frac{V_w}{V_{mem} + \lambda_{mem} * V_w} \tag{3.9}$$

$$E_{N_2} = 24 \tag{3.10}$$

$$scale_{N_2} = 8 \tag{3.11}$$

$$K_{N_2} = scale_{N_2} * (0.0295 + 1.21 * f_v - 1.93 * f_v^2) * 10^{-11} * e^{\frac{E_{N_2}}{R} * (\frac{1}{303} - \frac{1}{T_{stack}})} \tag{3.12}$$

Within the formulae above, the f_v is the volumetric ratio of water, E_{N_2} is the activation energy for nitrogen, $scale_{N_2}$ is a scale factor set to 8, R is the universal gas constant, and V_{mem} and V_w are the molar volumes of the dry membrane and liquid water respectively. Both T_{stack} and λ_{mem} are the same as explained earlier and are the stack temperature and the water content of the membrane respectively.

The above calculated flux is also per area and is thus multiplied by the area of a single cell and the total number of cells in the stack. The total transported nitrogen from the cathode to the anode is then used to determine the amount of nitrogen in the anode and cathode after the reaction, similar as for water.

3.5.3. Molar flows at the anode

The anode has three different species for which flows are determined. Firstly, the hydrogen flow into the anode is determined. The hydrogen flow at the exit of the anode is calculated by deducting the consumed hydrogen from the inflow as in equation 2.16. The consumed hydrogen for the stack in the second part of the equation is calculated as follows:

$$H_{2,min} = \frac{i + i_{loss}}{2 * F} * A_{cell} * n_{cells} \tag{3.13}$$

To dampen the oscillatory behaviour of the model, the calculated flows include a first order derivative. This has the effect that the amount of hydrogen in the stack varies over time. This is implemented in Simulink by adding a loop with an integrator as is shown in figure 3.9.

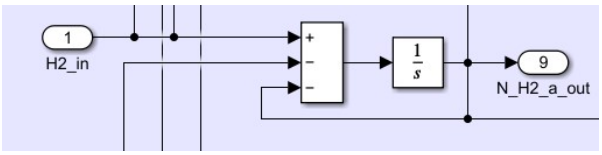

Figure 3.9: Hydrogen flow calculation with the integrator loop

Secondly, the water flow into the anode is determined based on the pressures in the cell and is calculated later on in the same molar flow model as is explained in section 3.5.5 in equation 3.14. The water flux calculated in the previous paragraph is then added to the inflow of water and the rate of change of hydrogen is deducted in order to calculate the flow of water at the anode exit. The first order derivative is implemented similarly to the calculation for the hydrogen exit flow as was shown in figure 3.9.

Thirdly, the nitrogen flow is modelled exactly the same as the water flow. The nitrogen inflow is dependent on the amount air needed for the power demand. Then the calculated nitrogen flux is added and a first order derivative is implemented to calculate the nitrogen flow at the exit of the anode.

3.5.4. Molar flows at the cathode

In the cathode there are five species of which the flows are to be determined. Firstly, the oxygen flow at the inlet is derived from the air flow and dependant on the requested power. The consumed oxygen is subtracted from the inlet flow. The consumed oxygen is determined via the consumed hydrogen. The oxygen consumption is a factor 0.5 of the consumed hydrogen. Lastly, the implementation of the first order derivative is similar to the implementation of the anode calculations.

Secondly, the water flow is present in the cathode as well as in the anode and is calculated similarly. The water at the inlet is calculated separately and will be explained in the section below (3.5.5). Then the water produced in the reaction will be added to the inlet flow and this is equal to the amount of consumed hydrogen. Thereafter the water that is transported from the cathode to the anode is deducted. The first order derivative is implemented similarly to the other species.

Thirdly, the nitrogen in the cathode is determined by subtracting the transported nitrogen from the inlet flow. The loop with the integrator to include the first order derivative, which is present in the other calculations, is left out because the nitrogen flow in the cathode is quite stable. A dampening loop would

mean additional computing which is unnecessary in this case.

Lastly, the carbon dioxide and argon flows are assumed to be non-reactive and are thus modelled so the exit flows equal the entry flows of the cathode.

3.5.5. Ratio of liquid and gas water

In the previous sections, the inlet flow of water was used in the calculations. The inlet flow is determined in these blocks together with the ratio of liquid and gas water at the inlets and exits of the anode and cathode. The amount of water in the liquid and in the gas phase are also used as inputs in the energy balance model. The implemented calculations to determine the ratio of water in gas phase and in liquid phase are from Yu et al. (2005).

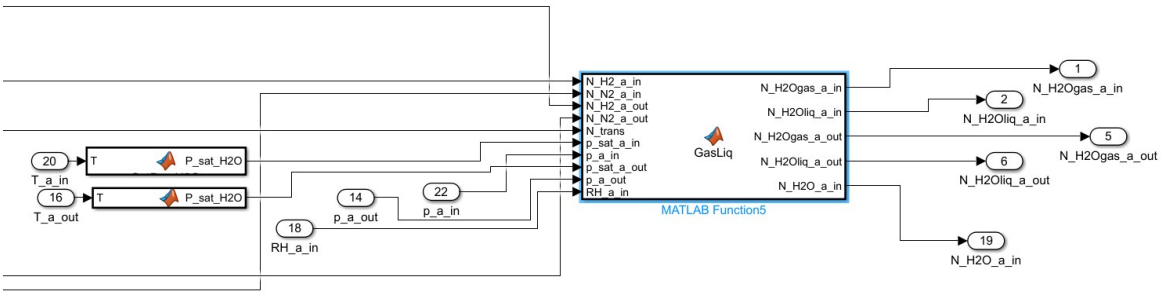

Figure 3.10: Gas and liquid ratio calculation block with inputs and outputs

Starting with the anode, the necessary input information consists of the amount of hydrogen ($\dot{N}_{H_2,a,in}$ and $\dot{N}_{H_2,a,out}$) and nitrogen ($\dot{N}_{N_2,a,in}$ and $\dot{N}_{N_2,a,out}$) at the inlet and exit of the anode, which were calculated in the first part of the molar flow model. The transported water ($\dot{N}_{trans}$) is already calculated as described in section 3.5.2. The pressures at the inlet ($p_{a,in}$) and exit ($p_{a,out}$) of the anode are input parameters and calculated in the pressures and partial pressures model (section 3.6) respectively. The saturated pressures ($p_{sat,a,in}$ and $p_{sat,a,out}$) are calculated first based on the temperatures at the inlet ($T_{a,in}$) and exit ($T_{a,out}$), which are a set parameter for the inlet and for the exit calculated in the energy balance model (section 3.7). Lastly, the relative humidity at the anode ($RH_{a,in}$) is needed for the calculations and is an input parameter which is theoretically controlled by the humidifier in the balance of plant, but was chosen to be constant in this model.
The calculation for the saturated pressures is done via the steam tables script written by Magnus Holmgren (Holmgren, 2023) and is shown as a preliminary step in figure 3.10.
The calculations inside the anode block start with the total amount of water flow at the inlet ($\dot{N}_{H_2O,a,in}$). This is calculated as follows:

$$\dot{N}_{H_2O,a,in} = \frac{(\dot{N}_{H_2,a,in} + \dot{N}_{N_2,a,in}) * p_{sat,a,in} * RH_{a,in}}{p_{a,in} - p_{sat,a,in} * RH_{a,in}} \tag{3.14}$$

Thereafter, the maximum amount of water in gas phase at the exit ($\dot{N}_{H_2O_{gas},max,out}$) is determined and the amount of gas and liquid at the entrance, which are also needed to determine the amount of gas and liquid at the exit of the anode. The amount of water in gas phase at the inlet is set to 100% due to the assumption that the all inflow is in gas phase; the amount of liquid water consequently is 0.

$$\dot{N}_{H_2O_{gas},max,out} = (\dot{N}_{H_2,a,out} + \dot{N}_{N_2,a,out}) * \frac{p_{sat,a,out}}{p_{a,out} - p_{sat,a,out}} \tag{3.15}$$

$$\dot{N}_{H_2O_{gas},a,in} = \dot{N}_{H_2O,a,in} \tag{3.16}$$

$$\dot{N}_{H_2O_{liquid},a,in} = 0 \tag{3.17}$$

The ratio of liquid and gas phase at the exit is dependant on the pressure and saturation, which is shown below (eq. 3.18):

$$\begin{matrix}\dot{N}_{H_2O_{gas},a,out} \\ \dot{N}_{H_2O_{liquid},a,out}\end{matrix} = \begin{cases} \dot{N}_{H_2O,a,in} - \dot{N}_{trans} & \text{if } p_{a,out} < p_{sat,a,out} \\ 0 & \\ \dot{N}_{H_2O_{gas},max,out} & \\ \dot{N}_{H_2O,a,in} - \dot{N}_{trans} - \dot{N}_{H_2O_{gas},max,out} & \text{elseif } \dot{N}_{H_2O,a,in} - \dot{N}_{trans} > \dot{N}_{H_2O_{gas},max,out} \\ \dot{N}_{H_2O,a,in} - \dot{N}_{trans} & \text{else} \\ 0 & \end{cases} \tag{3.18}$$

The input information necessary to complete the calculations at the cathode are the inflows and exit flows of oxygen and nitrogen, the amounts of transported and produced water, the pressures and saturated pressures at the inlet and exit, and the relative humidity at the inlet. The calculation block is shown below with the input variables included (fig. 3.11).

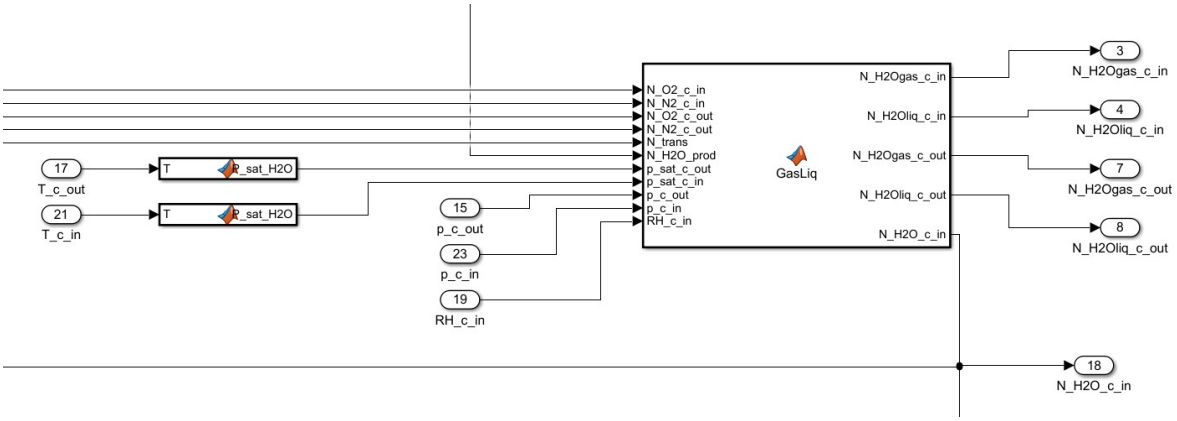

Figure 3.11: Gas and liquid ratio calculation block with inputs and outputs

The calculation for the total amount of water at the inlet of the cathode is shown below:

$$\dot{N}_{H_2O,c,in} = \frac{RH_{c,in} * p_{sat,c,in}}{p_{c,in} - p_{sat,c,in} * RH_{c,in}} * (\dot{N}_{O_2,c,in} + \dot{N}_{N_2,c,in}) \tag{3.19}$$

Thereafter, the ratio of the gas and water phase is determined by first calculating the maximum amount of gas at the inlet and exit and then the amount of liquid and gaseous water at both inlet and exit of the cathode similar to the anode.

$$\dot{N}_{H_2O_{gas},max,in} = (\dot{N}_{O_2,c,in} + \dot{N}_{N_2,c,in}) * \frac{p_{sat,c,in}}{p_{c,in} - p_{sat,c,in}} \tag{3.20}$$

$$\dot{N}_{H_2O_{gas},max,out} = (\dot{N}_{O_2,c,out} + \dot{N}_{N_2,c,out}) * \frac{p_{sat,c,out}}{p_{c,out} - p_{sat,c,out}} \tag{3.21}$$

$$\begin{matrix}\dot{N}_{H_2O_{gas},c,in} \\ \dot{N}_{H_2O_{liquid},c,in}\end{matrix} = \begin{cases} \dot{N}_{H_2O_{gas},max,in} & \text{if } \dot{N}_{H_2O,c,in} > \dot{N}_{H_2O_{gas},max,in} \\ \dot{N}_{H_2O,c,in} - \dot{N}_{H_2O_{gas},max,out} & \\ (\dot{N}_{O_2,c,in} + \dot{N}_{N_2,c,in}) * \frac{p_{sat,c,in} * RH_{c,in}}{p_{c,in} - p_{sat,c,in} * RH_{c,in}} & \text{else} \\ 0 & \end{cases} \tag{3.22}$$

$$\begin{matrix}\dot{N}_{H_2O_{gas},c,out} \\ \dot{N}_{H_2O_{liquid},c,out}\end{matrix} = \begin{cases} \dot{N}_{H_2O,c,in} + \dot{N}_{H_2O,prod} + \dot{N}_{trans} & \text{if } p_{c,out} < p_{sat,c,out} \\ 0 & \\ \dot{N}_{H_2O_{gas},max,out} & \\ \dot{N}_{H_2O,c,in} + \dot{N}_{H_2O,prod} + \dot{N}_{trans} - \dot{N}_{H_2O_{gas},max,out} & \text{elseif } \dot{N}_{H_2O,c,in} + \dot{N}_{H_2O,prod} + \dot{N}_{trans} \\ & > \dot{N}_{H_2O_{gas},max,out} \\ \dot{N}_{H_2O,c,in}\dot{N}_{H_2O,prod} + \dot{N}_{trans} & \text{else} \\ 0 & \end{cases} \tag{3.23}$$

3.6. Pressures and partial pressures model

Throughout the model the pressures or partial pressures of different species are used in calculations. The pressures and partial pressures are calculated in a separate block for both the exits and if necessary the inlets. The calculations are based on Yu et al. (2005)

3.6.1. The input and output variables

The input variables for the pressure and partial pressure calculations are the inlet and exit flows of all the species, the temperatures at the inlet and exit of both the anode and the cathode, and the pressures at the inlet of the anode and cathode. The temperatures at the exit are determined in the energy balance model block which will be explained hereafter. The pressure at the exit and the partial pressures which are calculated in this block are already used in the molar flow model block, thus creating a loop. This loop is broken using memory blocks, since they use the value of the previous iteration as explained in section 3.3. The overview of the input and exit variables is shown in figure 3.12 below.

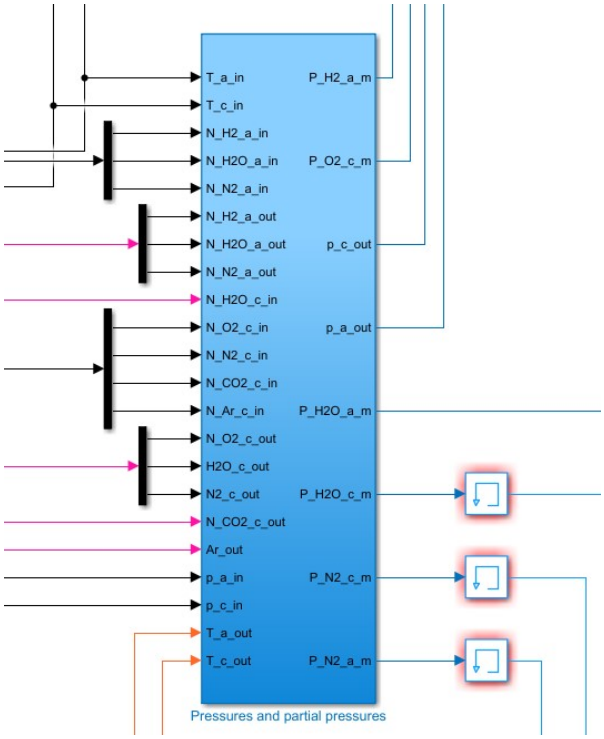

Figure 3.12: Overview of inputs and outputs of the pressures block

3.6.2. Calculation of velocity of gas inside cell

The pressure drop is calculated for the gas phase, not taking into account the phase change that may occur during the pressure drop. The first step in calculating the pressure at the exits is calculating the velocity of the gas inside the cell. The velocity of the gas is then used to determine the pressure drop. The necessary input information for the calculation are the relative humidities and saturated pressures of water at the inlet and exit which are calculated using the steam tables. Furthermore, the pressures at the inlet and exit, the temperatures at inlet and exit, and the hydrogen flow at inlet and exit are variables used in the calculation.
The calculation of the mean velocity of gas in the anode ($V_{a,m}$) is as follows:

$$\dot{N}_{in} = \dot{N}_{H_2,a,in} * (1 + \frac{p_{sat,a,in} * RH_{a,in}}{p_{a,in} - p_{sat,a,in} * RH_{a,in}}) \tag{3.24}$$

$$\dot{N}_{out} = \dot{N}_{H_2,a,out} * (1 + \frac{p_{sat,a,out} * RH_{a,out}}{p_{a,out} - p_{sat,a,out} * RH_{a,out}}) \tag{3.25}$$

$$V_{a,in} = \frac{\dot{N}_{in} * 22.4 * 10^{-3}}{A_{channel} * n_{channel}} * \frac{p_{atm}}{p_{a,in}} * \frac{T_{a,in}}{T_{ref}} \tag{3.26}$$

$$V_{a,out} = \frac{\dot{N}_{out} * 22.4 * 10^{-3}}{A_{channel} * n_{channel}} * \frac{p_{atm}}{p_{a,out}} * \frac{T_{a,out}}{T_{ref}} \tag{3.27}$$

$$V_{a,m} = \frac{V_{a,in} + V_{a,out}}{2} \tag{3.28}$$

The parameters used in the calculation are the reference temperature (T_{ref}), the atmospheric pressure (p_{atm}), the area of a single channel ($A_{channel}$), and the number of channels ($n_{channel}$). All parameters used in the calculations are given in Appendix B.

For the cathode, the calculation for the mean velocity of gas is similar to the calculation for the anode. Substitute for the hydrogen flow, the summation of oxygen and nitrogen flow. All other variables will be substituted by the corresponding variables for the cathode.

3.6.3. Calculation of pressure drop

The calculated mean velocity is used to determine the pressure drop. The pressure drop is calculated as follows assuming ideal gasses:

$$\Delta p_a = f_a * \frac{L_a}{D_a} * \frac{\rho_a * V_{a,m}^2}{2} \tag{3.29}$$

The parameters L_a, D_a, and ρ_a are the length of the channel, the diameter of the channel, and the density of the gas mixture respectively. The friction factor f_a is calculated beforehand and is dependant on the Reynolds number. The equation for the friction factor can be applied since it is assumed here that the flow in the channel is laminar. ν_a is the kinematic viscosity, this is calculated using the dynamic viscosity μ_a and the density of the gas.

$$\nu_a = \frac{\mu_a}{\rho_a} \tag{3.30}$$

$$Re = \frac{V_{a,m} * D_a}{\nu_a} \tag{3.31}$$

$$f_a = \frac{64}{Re} \tag{3.32}$$

The calculation of the pressure drop is again the same for the cathode. Afterwards, the pressures at the outlets of the fuel cell are calculated by subtracting the pressure drops from the inlet pressures at both the cathode and anode sides separately. The exit pressure calculation is followed by a memory block to break the loop created in the calculation of the velocity of the gas, as described in section 3.6.2.

3.6.4. Calculation of partial pressures

The partial pressures are calculated using the molar flows of all the species at the inlet of the anode. First the molar fraction of the flows are calculated and those fractions are then multiplied with the pressure in order to get the partial pressures.
The exact same method is used to calculate the partial pressures at the exit of the anode and at the inlet and exit of the cathode as well. The average of the inlet and outlet partial pressure is then taken to be used in the rest of the model. The partial pressures calculated are for the entire stack and not a single cell. The outlet pressures and mean partial pressures are used in the calculations of the electrochemical balance and the molar flow model.

3.7. Energy balance model

The energy balance model calculates the temperature increase of the fuel cell stack. The balance is made up of the electrical, theoretical, sensible, and latent heat, and of the heat loss and cooling. Each of these components will have their implementation discussed in more detail below.

3.7.1. Input and output variables

The input variables of the energy balance model are the temperatures at the inlets, the temperature and molar flow of the coolant, the current stack temperature, the molar flows at the inlets and outlets for all species including the distinction in gas or fluid water, the voltage, and the current density. The overview of the inputs and outputs of this submodel is shown in figure 3.13.

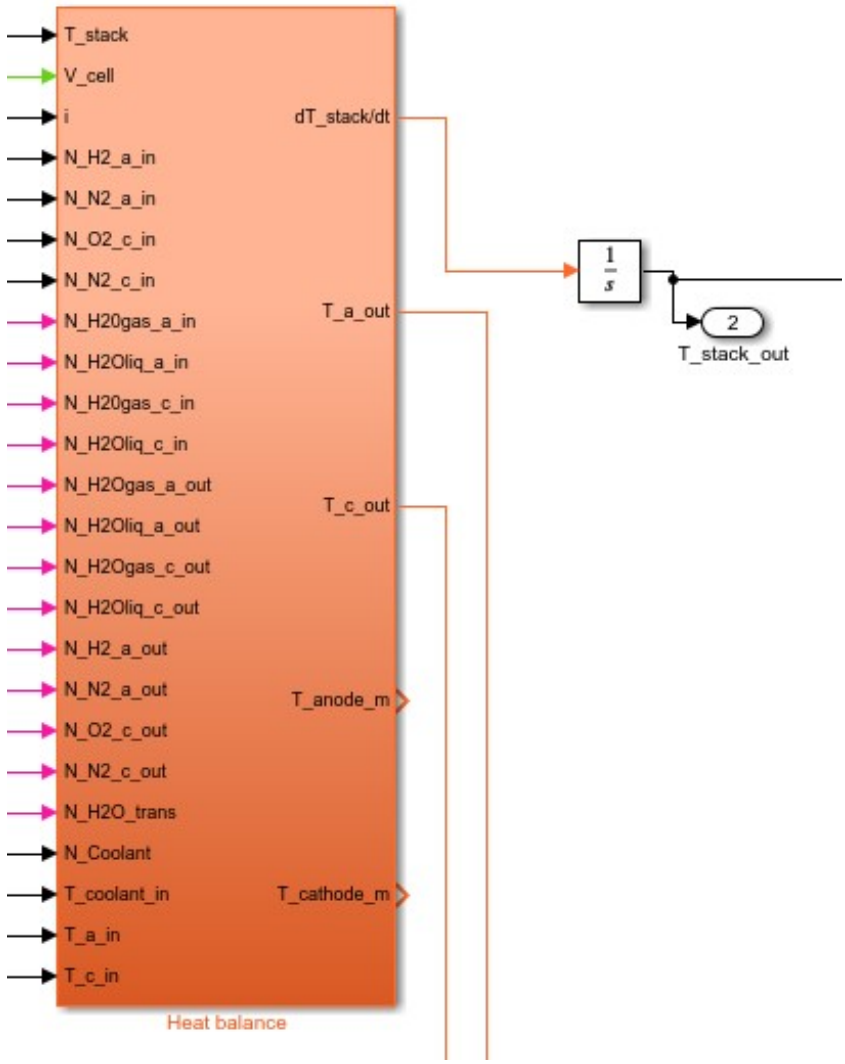

Figure 3.13: Overview of the inputs and outputs of the energy balance submodel

3.7.2. Temperatures at the outlet

The first step to calculate the different components of the energy balance model is to calculate the temperatures at the exit of the anode and cathode. The temperatures are necessary for the calculations of the sensible and latent heat.

The calculation of the temperatures at the exit requires the energy transfer due to mass transfer and mass converted in chemical reactions, the sensible heat, and the latent heat. The sensible heat and the latent heat values are calculated in section 3.7.5 and 3.7.6. These create loops which are resolved using memory blocks.

The energy due to mass transfer and mass converted in reactions is calculated as shown in equations 3.34 and 3.35:

$$q_{mass,a} = \dot{N}_{trans} * \Delta h_{H_2O_{gas}} + \dot{N}_{H_2,cons} * \Delta h_{H_2} \tag{3.33}$$

$$q_{mass,c} = \dot{N}_{trans} * \Delta h_{H_2O_{gas}} + \dot{N}_{H_2,cons} * \Delta h_{H_2O_{liquid}} - \dot{N}_{O_2,cons} * \Delta h_{O_2} \tag{3.34}$$

(3.35)

The molar flows are already calculated in the molar flow model and the enthalpy is calculated beforehand using the steam tables script. The consumed hydrogen ($\dot{N}_{H_2,cons}$) and oxygen ($\dot{N}_{O_2,cons}$) flows are derived from the inflows and exit flows by subtracting the inlet molar flow from the molar flow at the exit. The enthalpy of the water in gas phase ($\Delta h_{H_2O_{gas}}$) is calculated by adding the vaporisation

enthalpy (eq. 3.36) to the enthalpy of the liquid water ($\Delta h_{H_2O_{liquid}}$).

$$H_{vapor} = 45070 - 41.9 * T_{stack} + 3.44 * 10^{-3} * T_{stack}^2 + 2.54 * 10^{-6} * T_{stack}^3 - 8.98 * 10^{-10} * T_{stack}^4 \tag{3.36}$$

After calculating the energy due to the mass transfer and converted mass, the temperatures at the exit of the anode are calculated as follows:

$$T_{a,out} = 2 * (T_{stack} - \frac{q_{sens,a} + q_{latent,a} + q_{mass,a}}{hA_a}) - T_{a,in} \tag{3.37}$$

$$T_{c,out} = 2 * (T_{stack} - \frac{q_{sens,c} + q_{latent,c} - q_{mass,c}}{hA_c}) - T_{c,in} \tag{3.38}$$

This calculation is based on the assumption that the average temperature in the anode and cathode is equal to the the sum of the temperatures at the inlet and outlet divided by two. The average temperature is then set equal to the stack temperature minus the heat transfer. Rewriting that equation will give equations 3.37 and 3.38 with the assumption of the heat transfer coefficient (hA) being constant.

3.7.3. Electrical power

The electrical power is the first component of the energy balance. The electrical power is calculated as follows:

$$q_{elec} = n_{cells} * V_{cell} * i * A_{cell} \tag{3.39}$$

The voltage of a single cell was calculated in the electrochemical balance and is multiplied with the total amount of cells (n_{cells}), the current density (i) and the area of the cell (A_{cell}). This gives the electrical power of the entire stack.

3.7.4. Theoretical energy

The second component of the energy balance is the theoretical energy. The theoretical energy is the product of the chemical reaction energy and the consumed hydrogen. The consumed hydrogen is calculated by subtracting the molar flow of hydrogen at the inlet from the hydrogen molar flow at the outlet. The chemical reaction energy is the enthalpy of combustion of hydrogen and is equal to $28600 \frac{J}{mol}$. This is the higher heating value of hydrogen and is used since the hydrogen inlet flow is assumed to be in gas phase.

3.7.5. Sensible heat

The sensible heat is the third component in the energy balance. The sensible heat is calculated for the anode and cathode separately. The first step is calculating the enthalpy for all the species present at the anode and cathode at both the inlet and exit. This is done based upon the temperatures at the inlet and exit of the anode and cathode with the steam tables script (Holmgren, 2023). Thereafter, the enthalpy for every specimen is multiplied with the molar flow of that specimen giving the sensible heat for each specimen.
The total sensible heat for the anode and cathode are a summation of all the sensible heats of the respective species. For the anode this summation is shown below:

$$\begin{aligned} q_{sens,a} = {} & q_{sens,H_2,a,out} + q_{sens,H_2O_{gas},a,out} + q_{sens,H_2O_{liquid},a,out} + q_{sens,N_2,a,out} \\ & - q_{sens,H_2,a,in} - q_{sens,H_2O_{gas},a,in} - q_{sens,H_2O_{liquid},a,in} - q_{sens,N_2,a,in} \end{aligned} \tag{3.40}$$

The sensible heat calculation for the cathode is the same using the species present at the cathode. The total sensible heat is the sum of the anode and the cathode sensible heats.

3.7.6. Latent heat

The fourth component of the energy balance is the latent heat. The latent heat is calculated using the molar flows of the gas phased water at the inlets and outlets, the molar flow of water transported from the anode to the cathode, and the mean temperatures at the anode and cathode.
The assumption that all species at the inlet are in gas phase simplifies the calculation of latent heat

at the cathode. First, the vaporisation enthalpy for the anode and cathode are calculated. They are calculated using equation 3.36 using the mean temperatures from the anode and cathode respectively. Then the latent heat is calculated as shown below:

$$q_{latent,a} = (\dot{N}_{H_2O_{gas},a,out} - \dot{N}_{H_2O_{gas},a,in} + \dot{N}_{H_2O,trans}) * H_{vapor,a} \tag{3.41}$$

$$q_{latent,c} = (\dot{N}_{H_2O_{gas},c,out} - \dot{N}_{H_2O_{gas},c,in} - \dot{N}_{H_2O,trans}) * H_{vapor,c} \tag{3.42}$$

The total latent heat is then the summation of the anode and cathode latent heat.

3.7.7. Heat loss

The fifth component of the energy balance is the heat loss. The heat loss is is dependant on the stack temperature and the thermal resistance. The loss is calculated using Newton's law of cooling, dividing the temperature difference to the reference temperature (T_{ref}) by the thermal resistance ($R_{thermal}$).

$$q_{loss} = \frac{T_{stack} - T_{ref}}{R_{thermal}} \tag{3.43}$$

3.7.8. Heat loss due to cooling

The sixth component of the energy balance is the heat loss due to the cooling of the stack (q_{cool}). The cooling of the stack is modelled as a counter flow heat exchanger. The calculation is shown below in equation 3.44.

$$q_{cool} = \dot{N}_{cool} * C_{p,cool} * (T_{cool,out} - T_{cool,in}) \tag{3.44}$$

The molar flow of the coolant ($\dot{N}_{cool}$) is dependant on the stack temperature as the flow is determined using a feedback loop. The specific heat of the coolant ($C_{p,cool}$) is a parameter given in the parameter script (see Appendix B). The coolant temperatures at the inlet ($T_{cool,in}$) and outlet ($T_{cool,out}$) of the stack are set to a fixed temperature or calculated beforehand respectively. The control of the cooling is achieved by changing the coolant flow rate, and not by changing the temperature of the inflow of the coolant. The coolant temperature while exiting the fuel cell stack is calculated using the stack temperature, the heat loss due to cooling, and the coolant inflow temperature as is shown below. Herein, hA_{cool} is the heat transfer coefficient multiplied with the surface area where the heat transfer takes place. This parameter is often taken as a single value when determined experimentally.

$$T_{cool,out} = 2 * (T_{stack} - \frac{q_{cool}}{hA_{cool}}) - T_{cool,in} \tag{3.45}$$

The heat loss due to cooling is the same as calculated in equation 3.44 and uses a memory block to break the algebraic loop this creates.

3.7.9. Energy balance and calculation of the stack temperature

After calculating all six components of the energy balance, the temperature change over time can be calculated with the differential equation shown below (eq. 3.46). This is also the only differential equation considered in the model.

$$\frac{dT_{stack}}{dt} = \frac{q_{theo} - q_{elec} - q_{sens} - q_{latent} - q_{loss} - q_{cool}}{m * C_{p,stack}} \tag{3.46}$$

The mass times specific heat is a stack parameter dependent on the size of the stack. In this case the $m * C_{p,stack}$ is estimated at 4600 J/K.
The stack temperature is then calculated by integrating the temperature change over time. In Simulink the integrator block is used to implement the integration in the model.

3.8. Fuel cell stack outputs and control

The remaining calculations within the fuel cell stack are the power output that is generated by the stack and the relative humidities at the anode and cathode. The power output of the stack is calculated by

multiplying the voltage calculated in the electrochemical model with the amount of cells in the stack. Thereafter, the stack voltage is multiplied with the current to determine the stack power.

The relative humidities are calculated using the stack temperature and the partial pressure of water for the anode and the cathode separately. The relative humidities are then used to calculate the membrane water content which was used in the electrochemical model and the molar flow model. The relative humidities are determined by dividing the partial pressure by the saturated pressure of water. The saturated pressure is determined via the temperature in the steam tables script.

The power output is the desired output and determines the input molar flows of the operation. The stack power output is compared to the required power and the difference herein determines the input current and thus the input hydrogen and air molar flows. The feedback loop for stack power uses a standard PID controller to control the input current to gain the required output voltage.

The second feedback loop is the cooling of the stack. As briefly discussed in section 3.7.8, the cooling of the fuel cell stack is controlled by changing the coolant flow. The stack temperature is compared to a preset target temperature at which the fuel cell theoretically should work the most optimal and this difference is the input for adapting the coolant flow. A standard PID controller is used in this feedback loop as well to dampen the change in coolant flow rate. The coolant flow is changed to keep a constant temperature difference between coolant inflow and exit flow temperatures.

The PID controllers have not been tuned in a systematic approach; values were manually selected to obtain controllers that are capable of regulating the current and the coolant flow.

4

Results

In this chapter, first the results will be discussed in terms of efficiency of the model. Then three different test cases are shown and lastly the validation and verification of the model will be discussed. The three test cases are simplified situations which could occur on a ship. They are summarised in an abrupt decrease in power, a steady increase in power, and a varying demand during a longer time period.

4.1. Efficiency discussion

In order to check the feasibility of the model, the efficiency of the modelled fuel cell stack is checked in order to compare this with the expected efficiency. Beforehand the mass balance and the energy balance are set up in order to heck if the conservation of mass and energy are correctly modelled.

First, the data is extracted from the model concerning the molar flows into and exiting the stack at a timestep after reaching steady state. These molar flows are then converted into mass flows. The mass flows in and out are summed and compared to discern if the conversion of mass is correctly modelled. The mass balance, shown in blue in figure 4.1, indicates that the conversion of mass is correctly modelled since the difference between the inflow is 0.0009 percent, which is negligible.

Molar Balance		
	In [g]	Out [g]
H2 anode	0,009176693	0,002889236
H2O anode	0,001451059	0,061873705
N2 anode	0	4,79093E-05
O2 cathode	0,305103201	0,255202822
H2O cathode	0,019273437	0,015051212
N2 cathode	0,99592325	0,99587534
total	1,33092764	1,330940224
difference	-1,25838E-05	grams
	-0,0009455%	

Energy Balance			
In	[W]	Out	[W]
Theoretical energy	891,9706373		
		Electrical energy	700,000433
		Sensible heat anode	129,399161
		Sensible heat cathode	136,918295
		Latent heat anode	0
		Latent heat cathode	96,1934574
		Heat loss	3,22647059
		Cooling loss	-173,766424
total	891,9706373		891,971393
difference	-0,000755524	W	
	-0,0000847%		

Figure 4.1: Mass balance (blue) and energy balance (red) for a single timestep after reaching steady-state

Thereafter, the energy balance of the model, shown in red in figure 4.1, is also checked for the conversation of energy. The theoretical energy is what is produced by the hydrogen and oxygen forming water. This is the input energy from which the energy losses are subtracted resulting in the electrical

energy. The input energy should be equal to the sum of the losses and useful energy output. In this case, they are equal with a negligible difference of 0.00008 percent.

The efficiency of the fuel cell stack depends on multiple factors. The efficiency in this case is defined as:

$$\eta = \frac{P_{elec}}{P_{theo}} * 100\% \tag{4.1}$$

An influential parameter is the (requested) stack temperature. The temperature in the stack determines the heat loss in sensible and latent heat and the loss due to necessary cooling. A too high temperature results into higher losses and thus a lower efficiency. However, too low a stack temperature has a lower efficiency as well, because proton conductivity and the exchange current density are decreased with the temperature as is explained by L. Wang et al. (2003).

The optimal temperature for the highest efficiency is found to be around 80 degrees Celsius. When running the model with the requested stack temperature at 80 degrees Celsius, the efficiency is roughly at 70 till 80 percent depending on the power demand. These efficiencies are in the expected range for PEM fuel cells. At 80 degrees Celsius, the stack is heated by the cooler due to the internal temperatures not reaching the set temperature of 80 degrees. The heating by the cooler works as an additional energy input to counter the increase in energy losses via the latent and sensible heats. This does explain why the efficiency does not change even though there should be higher losses at higher power outputs.

The figure below (4.2) shows the efficiencies at the different power demands ranging from 100 Watt to a 1000 Watt.

Power output [W]	Stack voltage [V]	Efficiency	Consumed H_2 [mol/s]
100	44,48	71%	-0,00049
200	43,24	76%	-0,00092
300	42,62	77%	-0,00136
400	42,27	78%	-0,00180
500	42,06	78%	-0,00224
600	41,93	78%	-0,00268
700	41,84	78%	-0,00312
800	41,77	79%	-0,00356
900	41,71	79%	-0,00400
1000	41,66	79%	-0,00444

Figure 4.2: Range of efficiency at different requested power outputs at 80 degrees Celsius

4.2. Test case: step response

The first test case is to simulate a sudden decrease in the requested power in order to see the reaction of the fuel cell stack. The test case is set to have a power decrease from 1000 to 400 Watt. This test case is chosen in order to simulate the case where there is a sudden unexpected failure and the power needs to be cut off directly from the failed equipment. This thus results in a lower demand for power.

Looking at the results after running the simulation with this test case, it is apparent that the fuel cell stack in itself is near instantaneous in switching to new power demands. The supply of oxygen, hydrogen, and coolant are all modelled to be instantaneous in switching the amount of flow. This is not realistic since the delays occurring in the system, which would affect the time till steady state, would mainly be in the balance of plant which is not modelled here.

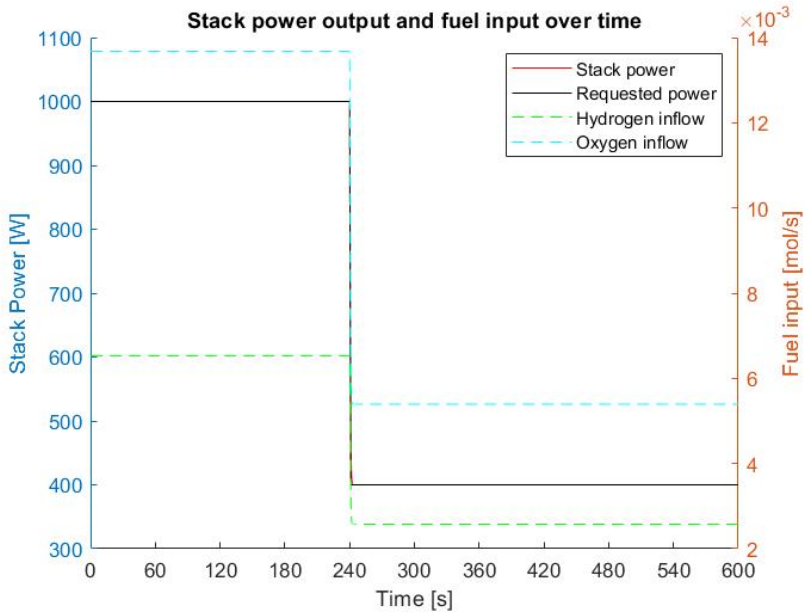

Figure 4.3: Reaction of hydrogen and oxygen inflow in response to a change in requested power from 1000 W to 400 W

In the figure above (4.3) the requested power was changed from 1000 W to 400 W after 240 seconds. The figure shows the change in inflow of hydrogen and oxygen over time as well. This shows the time it takes for the system to reach steady state again. The current model reaches steady state in roughly three seconds after the change in power demand. The inflows are directly related to the current and change with the same speed as the current is changed to accommodate the lower power demand. The power output is equal to the demand after a few seconds as well. Modelling the missing balance of plant equipment, such as the pumps and pressure valve, would give realistic delays in reaching steady state.

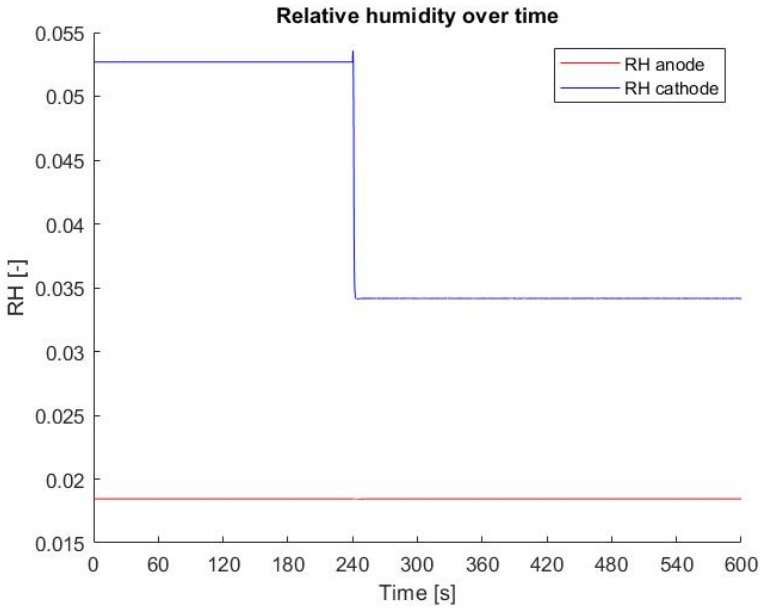

Figure 4.4: Change in relative humidity at the anode and cathode in response to a change in requested power from 1000 W to 400 W

Figure 4.4 shows the response of the relative humidity at the anode and the cathode over time. It can

clearly be seen that the relative humidity on the cathode side decreases after the first 240 seconds. This is due to the fact that less water is created in the electrochemical reaction at a lower power production. The produced water is formed at the cathode side explaining why only at the cathode side a decrease in relative humidity is visible due to the lower power output.

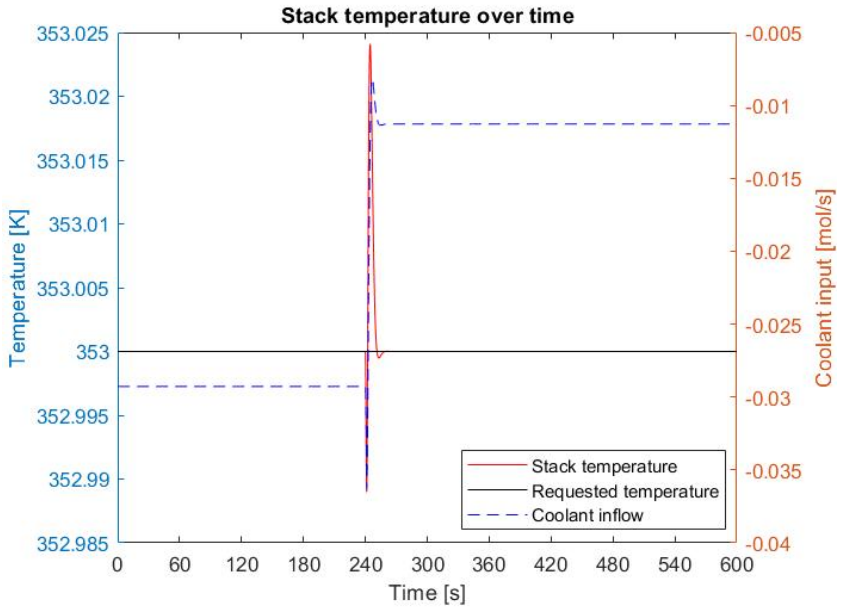

Figure 4.5: Change in stack temperature and coolant flow in response to a change in requested power from 1000 W to 400 W

The temperature change in the stack due to a decrease in power demand is not significantly present as can be seen in figure 4.5. The temperature change is limited to 0.02 degrees Kelvin which is a negligible difference. What can be seen from this small change in temperature is that the temperature rises as a response to a decrease in power demand contrary to the expectation that the temperature would decrease. A possible explanation for this increase in temperature is a shift in the distribution of theoretical power. It could be that the decrease in demanded electric power results in the increase of latent and sensible heat while keeping the total amount of theoretical power the same. The increase in produced heat would heat up the fuel cell stack.

The coolant inflow is negative in this simulation. This would mean in this case that the temperature due to generated heat is lower than the requested stack temperature and therefore the cooler is acting as a heater. Negative flows are the result of the mathematical model of the heat exchanger and are not realistic. The coolant flow after the decrease in power demand is still negative, but is moving closer to zero. This means that there is less heating needed to reach the set temperature.

In addition to the temperature discussion, it must be noted that the control of the temperature is near perfect to the point of regulating the temperature to a tenth of a degree. In a physical set-up, the temperature regulation would most likely not be based on a sensor directly in the stack, but on temperatures exiting the stack or the heat exchanger. The accuracy of the temperature sensor should also be taken into account. While there might be sensors which can achieve the precision as shown in the model, it is not necessary to use them in reality, because it will not practically have any effect on the operation of the fuel cell stack in a ship.

The conclusion of this test case is that the behaviour of the modelled fuel cell stack is as expected with regards to the changes in inflows and relative humidity. The stable temperature throughout the entire simulation is unexpected. A bigger change in temperature at the time of the step in power demand was expected in combination with a higher coolant flow after the step in power demand. A higher cooling flow could have been the outcome if the generated heat was high enough for the system to

need cooling.

4.3. Test case: linear increase from 100 W to 1000 W

The second test case is a steady increase in power demand from 100 Watt to a 1000 Watt over the course of 10 seconds to simulate starting up the fuel cell at the start of the voyage of the ship. This test case starts at 100 Watt as the model becomes unstable below this power setpoint.

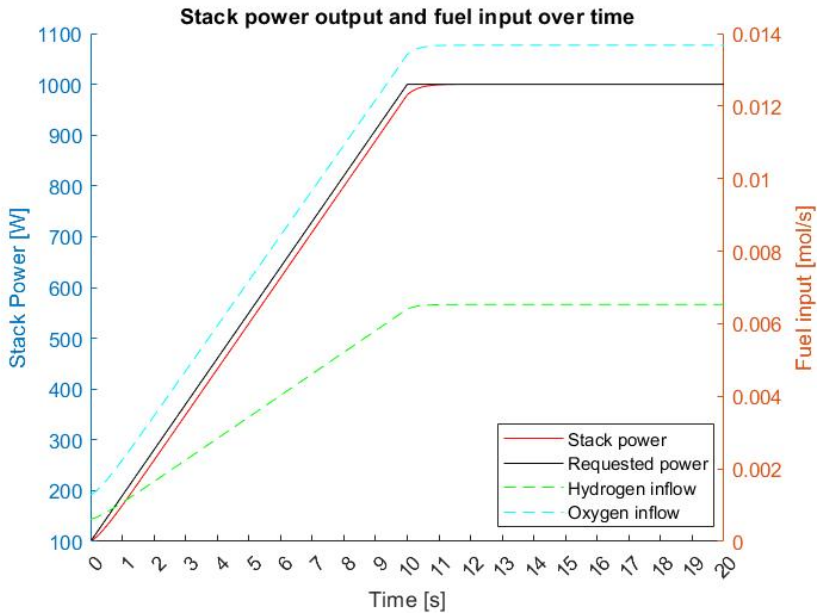

Figure 4.6: Reaction of hydrogen and oxygen inflow in response to a linear increase in power demand from 100 W to 1000 W

The first figure (4.6) shows the change in power and requested power over time including the corresponding molar flows of hydrogen and oxygen. As can be seen in the figure, the inflows are adapting to the change in power demand near instantly, as was the case with the first test case.

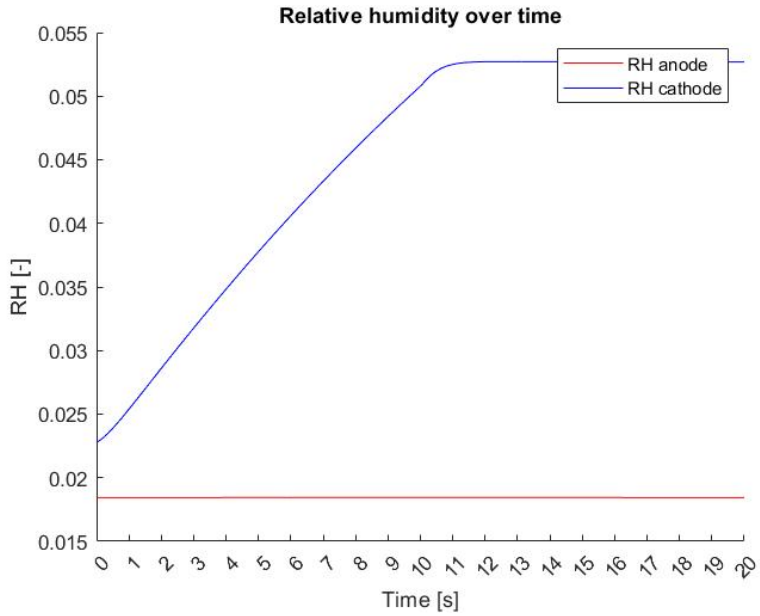

Figure 4.7: Change in relative humidity at the anode and cathode in response to a linear increase in power demand from 100 W to 1000 W

The relative humidity on the anode and cathode side over time are shown in figure 4.7. The relative humidity at the anode side stays the same independent of the change in power output. This is due to the temperature not changing either as can be seen in figure 4.8. The relative humidity on the cathode side is steadily increasing as the production of water in the electrochemical reaction increases along with the power output.

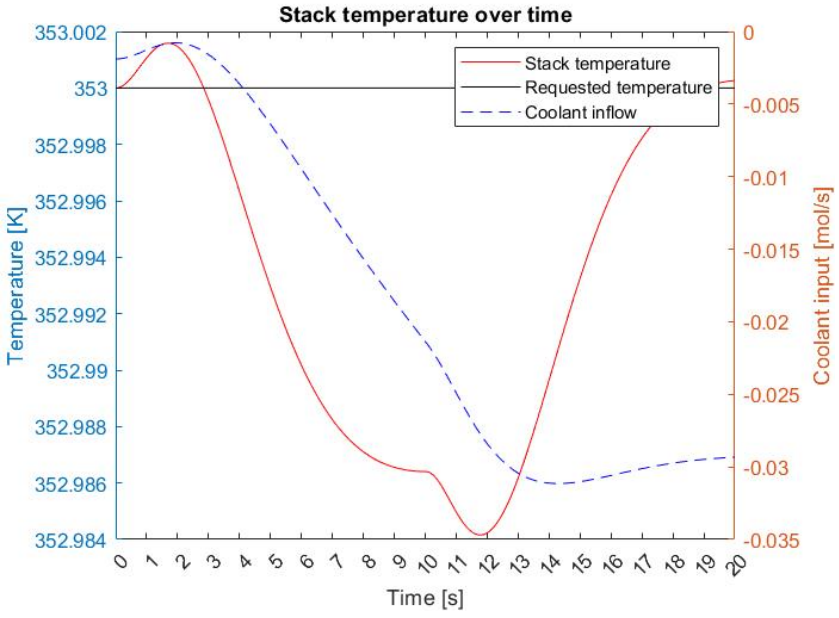

Figure 4.8: Change in stack temperature and coolant flow in response to a linear increase in power demand from 100 W to 1000 W

The temperature unexpectedly drops during the simulation as shown in figure 4.8. The requested temperature is set to 353 Kelvin since this should give the highest efficiency. However, this set temperature results in a situation where there is no additional cooling necessary. In fact, the way the system is im-

plemented unrealistically results in negative cooling flows, which heat up the system instead of cooling it due to the pure mathematical set up. The changes in coolant flow and temperature are close to zero during the entire simulation, meaning that the temperature change is in fact negligible.

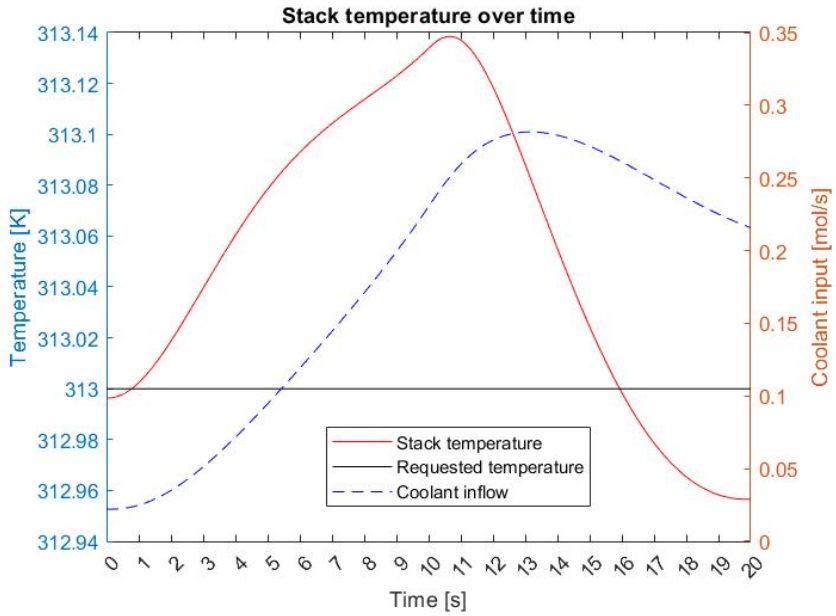

Figure 4.9: Change in stack temperature and coolant flow in response to a linear increase in power demand from 100 W to 1000 W at 313 K

The same simulation is run with the requested temperature lowered to 313 Kelvin. The lower temperature results in the need for additional cooling as is shown in figure 4.9. The coolant inflow is increasing as the power output and thus the heat generation increases for the ten seconds the power demand is increasing. After the 1000 Watt has been reached, the temperature and the coolant flow are decreasing again to eventually settle at the requested temperature.

The conclusion to this test case is that the output power follows the requested stack power during the simulation. The behaviour of the fuel cell is as expected with regards to the power output and the relative humidities. The behaviour of the temperature and the coolant flow depend on the set temperature. The gives the conclusion that the cooler acts as a heater at the original requested temperature and that the fuel cell loses too much heat passively to stay at operating temperatures.

4.4. Test case: Maritime duty cycle of an inland vessel

The third test case will be answering the last of the research questions, namely the affect of a maritime duty cycle on the fuel cell operation. The ship looked at for this test is an inland cargo vessel during a trip upriver on the Rhine with several locks during the second half of the journey. The maritime duty cycle of the inland cargo vessel test case is based on the example from Mariko GmbH and FME (2018). The inland ship from the example has a maximum power of 1100 kW. The current model only simulates a single stack and has therefore a set maximum power output of 1.1 kW. The duty cycle in this test case is shown for a single stack under the assumption that the total power of 1100 kW can be reached by adding a 1000 similar stacks together to output the requested power. The simulation is fourteen hours since that is an average workday taking into account the laws with respect to sailing hours. The power demand when the ship is in a lock is set to 100 kW, since the power source is usually not fully turned off during locking, but put on a low power while disconnecting the propellers. This also avoids the model getting to close to zero with several variables which could cause singularities in the simulation.

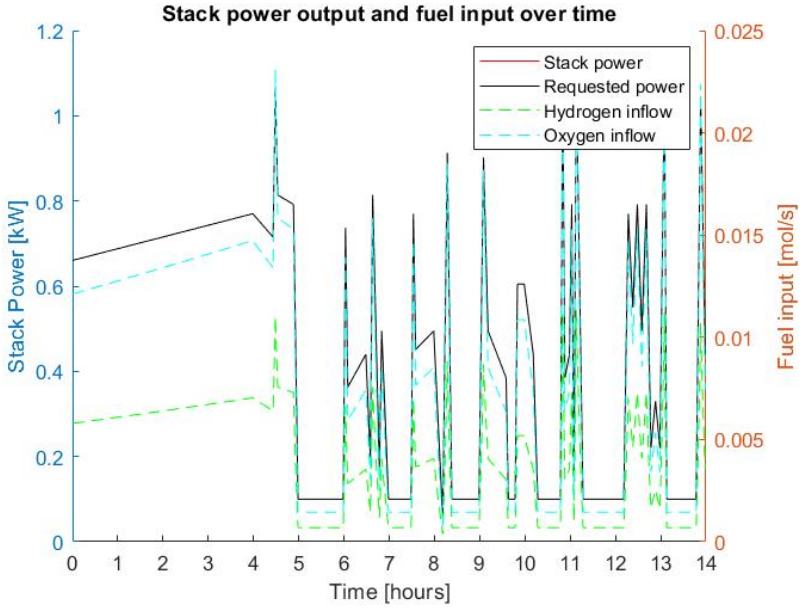

Figure 4.10: Stack power and the corresponding fuel input during the maritime duty cycle of the inland vessel

The figure above shows the power output with the corresponding hydrogen input and oxygen input flows. The power output changes during the voyage due to changing demand in way of locks. The hydrogen and oxygen flows adapt to the changing power demand. The time scale used in the figure is too big to accurately determine the details. However, the figure does illustrate the range in input flows for the maritime cycle. The hydrogen and oxygen flows for the modelled set up of maximally 1100 Watt range up to 0.015 and 0.025 mol/s respectively. For the test case of the inland vessel these values should be multiplied by 1000 to attain the requested power outputs.

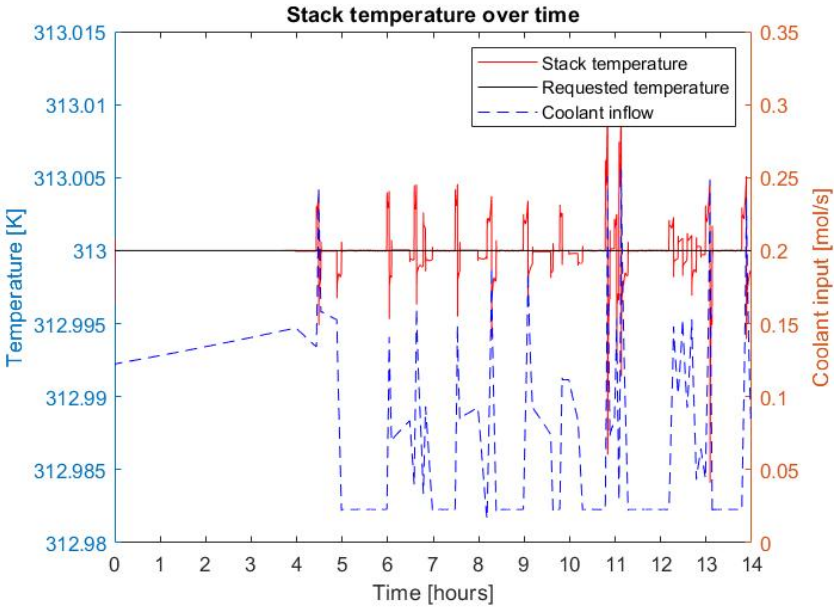

Figure 4.11: Temperature and coolant flow during the maritime duty cycle of the inland vessel

The temperature in the fuel cell is kept constant throughout the simulation in this case at 40 degrees Celsius as is shown in figure 4.11. The lower requested temperature ensures a positive and realistic

coolant flow. The coolant flow strongly responds to the minimal changes in temperature with the inflows ranging from near 0 to 0.25 mol/s. When taking into account that the coolant flow is for a single fuel cell stack, and thus would need to be multiplied by 1000, the amount of cooling and the strong response to temperature change could pose a problem. The heat exchangers and the pumps in the system would need to process several litres of coolant per second to meet the requested coolant flows for this situation. The exact amount of flow in litres is dependent on the actual coolant chosen.

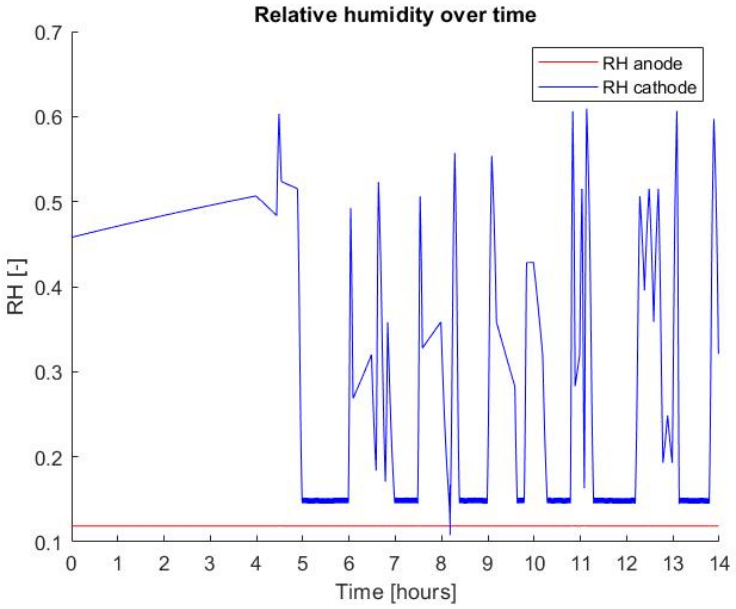

Figure 4.12: Relative humidity during the maritime duty cycle of the inland vessel

In figure 4.12, the relative humidities are shown for the anode and cathode during the simulated voyage. The relative humidity at the anode side stays constant as the relative humidity of the inflow is set to be constant and the water formed during the power production is formed at the cathode side. This means that the relative humidity at the cathode is constantly changing during the simulation as a consequence of the changing power demand. The range of the relative humidity at the cathode is roughly 0.15 to 0.6. This range is within the realistic expectations of a fuel cell. The relative humidity is not being regulated in this model, which could be done by adding a humidifier in the balance of plant to regulate the relative humidity of the oxygen inflow. Regulating the relative humidity of the inflow to maintain a more constant relative humidity in the fuel cell will help to keep the membrane water content at the desired level. This will prolong the life of the membrane.

The conclusion drawn from the third test case is that the flow changes behave as expected corresponding with the changes in power demand. This was also seen in the first two test cases and still apply during a 14 hour long simulation with several changes in power demand. The important result in this test case is the temperature changes. The temperature reacts strongly to the sudden spikes in the power demand, but less so to gradual changes, whereas the coolant flow change follows the power demand change without overshoots. This implies that the temperature control is more sensitive to power changes than the molar flow control.

4.5. Validating the model

After creating the model, the first step is to validate the model. The validation of the model is done by comparing the results from this model with other publications. The articles chosen to compare this model with, have their own model validated with an experimental set-up.

4.5.1. Comparing to Amphlett et al. model

In order to compare this model to the results from Amphlett et al. (1996), a simulation was run with their parameter set. This parameter set results in this model becoming unstable due to encountered singularities, which cannot be solved by Simulink's solvers. This singularity manifests in the implicit time integration within the first few timesteps of the simulation. This may indicate that the initial values do not represent a system (close to) equilibrium for this model. The solver is then unable to overcome this imbalance. As the model does not run to completion, it is not validated against the model of Amphlett et al. (1996).

4.5.2. Comparing results to Musio et al. steady state model

Similarly, the model was run with the parameters from Musio et al. (2011) in order to check if this parameter set is within the working limits of the model. The first obstacle in comparing the model to the results from the paper by Musio et al. (2011), is the lack of information about the used parameters. Besides the stack size, membrane type, and cell area, there are not a lot of parameters given. This means that most of the parameters were estimated and thus the results are less suitable for validation.

The results gained with the parameters from Musio et al. (2011) are not in line with the the results displayed in the paper. For example, the hydrogen inflow is, after converting the values to have the same units, almost two times higher than in the model than in the paper from Musio et al. (2011).

4.5.3. Conclusion to validation

In conclusion, the model is not validated. Either the input parameters were incomplete, or the model did not run to completion with the provided input parameters.
The next step will be to check if the results gained while running my model with the parameter set within the workable limits are feasible.

4.6. Reliability of the model

In order to verify the model, the model was set to run with a systematically varied set of input parameters to observe the change in the model's behaviour. During the verification it became apparent that the model is highly sensitive to variations in input parameters. Often, a slight change in a single input parameter resulted in an unstable model. The results that will be shown in the coming paragraphs are therefore not verified.

5

Conclusion and Recommendations

5.1. Conclusion

In the introduction, the research objective and the supporting research questions were posed. The research objective of this thesis is to simulate the dynamic behaviour of a proton exchange membrane fuell cell system. A fuel cell system consists of the fuel cell stack and the auxiliary components of the balance of plant. The auxiliary components consist of: 1) A heat exchanger to control the temperature of the fuel cell stack. 2) A humidifier to regulate the humidity of the inflow and thereby the humidity in the fuel cell. 3) An air compressor to control the operating pressure of the stack and flow rate and 4) an air cooler to regulate the inflow temperature of air.

The current model is a lumped parameter model that simulates the fuel cell stack and heat exchanger. The complete stack is assumed to consist of multiple identical fuel cells, because the overall performance of the fuel cell stack is of interest for this research and not the interaction between individual fuel cells. A lumped parameter model is suitable for this approach. The model for the fuel cell is based on the work of Rabbani and Rokni (2013), Yu et al. (2005), Del Real et al. (2007), and Amphlett et al. (1996) and implemented in Simulink, the simulation environment of MatLab. Additional components of the balance of plant (humidifier, air compressor and air cooler) are not included as the current model is often unstable.

Expanding on the existing literature, this model is implemented within Simulink. Simulink is a general purpose modelling environment, which would enable relatively easy coupling with other systems when integrating the fuel cell system with for example the entire drive train. The solvers offered by Simulink are therefor also general purpose and may not be suitable for the fuel cell stack model.

The current model is not validated or verified, but is tested with three test cases: 1) a step response, 2) linear increase in power demand and 3) maritime duty cycle of an inland vessel sailing up the river Rhine. As mentioned before, the current model is often unstable depending on the used input parameters. In general, for the stable simulations, it is observed that the power output follows the requested power demand closely. The change in power, temperature, hydrogen and oxygen flow, and coolant flow is near instantaneous. This is likely due to not implemented auxiliary components, which would add delays to the system. In addition, the imbalance of mass and energy is 0.0009% and 0.00008% respectively, which is negligible. Thus the current model correctly conserves mass and energy.

On the other hand, the current model is highly sensitive to variations in input parameters. This manifests itself as singularities during time integration of the heat equation. This sensitivity is also noticeable in the test cases with regards to temperature control. There is a distinct set of setpoint temperatures for the fuel cell stack for which the model is stable.

5.2. Recommendation for further research

The current model requires additional improvements to be able to assess the application of fuel cell systems in the maritime industry. Currently, it presents a starting point upon which can be expanded with further research.

The first point of recommendation is to improve the model's stability. Potential improvements are: 1) use of additional time-dependent differential equations for modelling (sub)systems. Currently, the model mostly consists of algebraic expressions which may present a difficult system to solve within each timestep. 2) Numerical modifications such as limiters to prevent large sudden changes that may introduce instability.

The second point of recommendation is to validate the model of the fuel cell stack to an experimental test set-up. This could give better insight in model parameters which were assumed in this model.

The third point of recommendation is to expand on the model to include the balance of plant. As was discussed, the key components of the balance of plant are the heat exchanger, humidifier, air compressor, and air cooler. Since these components are integral for the operation of the fuel cell, they should be added to the model for the accurate simulation of the fuel cell system. The expectation is that the balance of plant will ensure more delays in the system. First of all, the more realistic modelling of the heat exchanger to include a pump to change the coolant flow rate will give slower coolant flow rate changes and thus delays in the heat management of the fuel cell stack. Secondly, adding the balance of plant components that regulate the inflows of fuel and air will give both delays and more control options for the system. For example, the air flow will be regulated with a compressor, humidifier and a cooler. This gives more delays in changing the air flow rates, but also the temperature, pressure, and the relative humidity of the air at the inlet are changeable with their own control delays. The same situation arises for the fuel input. Depending on the exact balance of plant components which are added, the fuel input parameters are controllable. While there are more delays in the system which makes the power output control and the temperature control more difficult, it will also give the opportunity to incorporate the inflows as part of the heat management instead of only the stack cooler. An added benefit would be the regulation of water content of the fuel cell membrane via the relative humidity of the inflows to ensure the fuel cell is operating within its limits to prolong the working life duration.

The model in a complete state would be beneficial for the maritime industry to explore the possibilities of using a fuel cell system in current and future designs. This is due to the additional insight in the auxiliary components and their effect on the fuel cell stack, which makes it possible to decide beforehand if a fuel cell system will fit the intended operation of the ship.

Nomenclature

Abbreviations

IMO	International Maritime Organisation
NOx	Nitrogen-Oxides
PEM(FC)	Proton membrane exchange (fuel cell)

Subscripts

a	Anode
act	Activation
amb	Ambient
atm	Atmospheric
c	Cathode
$cell$	For a single fuel cell
$channel$	Of a channel
CO_2	For carbon-dioxide
$cons$	Consumed
$cool$	Cooling
e	Electrical
$elec$	Electrical
$g,\ gas$	In gas phase
H_2	For hydrogen
H_2O	For argon
H_2O	For water
in	At the inlet of the fuel cell
ion	Ionic
$l,\ liquid$	In liquid phase
$latent$	Latent
$mass$	Due to mass transfer and mass conversion in reactions
mem	(Dry) membrane
mem	Membrane
N_2	For nitrogen
O_2	For oxygen
$Ohmic$	Ohmic, following Ohm's law
out	At the outlet of the fuel cell
sat	Saturated

$sens$ Sensible

$stack$ For the entire fuel cell stack

th Thermal

$theo$ Theoretical

$trans$ Transported

$vapor$ Vaporisation

w For water

Greek symbols

α Transfer coefficient

β Symmetry factor for i_0

η Efficiency

μ_a Dynamic viscosity

ν_a Kinematic viscosity

ρ Density

Symbols

ΔG^0 Gibbs free energy

$\Delta H_{reaction}$ Enthalpy of combustion for hydrogen

Δ_λ Membrane water content coefficient

Δ_w Water diffusion coefficient

$\dot{N}$ Molar flow

λ Water content

$\overline{g}_f^0$ Specific Gibbs free energy

A Area

$a,\ a_w$ Activity of water

$C1$ Constant, 180

$C2$ Constant, 16.4

C_p Specific heat

D_a Diameter of a cell channel

E Theoretical fuel cell potential

e^- Electron

E^0 Ideal fuel cell potential

E_{N_2} Activation energy for nitrogen

F Faraday's constant

f_a Friction factor

f_v Volumetric ratio of water

H^+ Hydrogen ion

H_2 Hydrogen

hA	Heat transfer coefficient
i	Current
i_0	Exchange current density
i_{loss}	Fuel crossover and internal current generation losses
J	Flux
K	Permeation factor
k	Reaction rate coefficient for i_0
L_a	Length of cell channel
M	Molecular weight
m	Mass
n	Number of electrons
N_{cells}	Number of cells in the stack
$n_{channel}$	Number of channels in cell
n_{drag}	Electro-osmotic drag
$n_{e,a}$	Number of electrons used in reaction for anode, 4
$n_{e,c}$	Number of electrons used in reaction for cathode, 1
O_2	Oxygen
$P,\ p$	Pressure
P_0	Standard pressure
P_i	Partial pressure of the gases
q	Energy
R	Universal gas constant
r	Resistance
Re	Reynolds number
RH	Relative humidity
S	Stoichiometric ratio
$scale_{N_2}$	Scale factor for nitrogen, 8
T	Temperature
t	Thickness
T_0	Reference or room temperature
V	Voltage
V_a	Velocity of gas in the anode
V_c	Velocity of gas in the cathode
V_{mem}	Molar volume of dry membrane
V_w	Molar volume of liquid water
W	Work

Bibliography

Amphlett, J. C., Mann, R. F., Peppley, B. A., Roberge, P. R., & Rodrigues, A. (1996). A model predicting transient responses of proton exchange membrane fuel cells. *Journal of Power Sources*, *61*, 183–188. https://doi.org/10.1016/S0378-7753(96)02360-9

Del Real, A. J., Arce, A., & Bordons, C. (2007). Development and experimental validation of a pem fuel cell dynamic model. *Journal of Power Sources*, *173*, 310–324. https://doi.org/10.1016/j.jpowsour.2007.04.066

Holmgren, M. (2023). *X steam, thermodynamic properties of water and steam.* https://www.mathworks.com/matlabcentral/fileexchange/9817-x-steam-thermodynamic-properties-of-water-and-steam

Jia, J., Li, Q., Wang, Y., Cham, Y. T., & Han, M. (2009). Modeling and dynamic characteristic simulation of a proton exchange membrane fuel cell. *IEEE Transactions on Energy Conversion*, *24*, 283–291. https://doi.org/10.1109/TEC.2008.2011837

Mariko GmbH and FME. (2018). *Perspectives for the use of hydrogen as fuel in inland shipping* (tech. rep.). European Union.

Moran, M. J., Shapiro, H. N., Boettner, D. D., & Bailey, M. B. (2012). *Principles of engineering thermodynamics* (8th). John Wiley Sons.

Musio, F., Tacchi, F., Omati, L., Stampino, P. G., Dotelli, G., Limonta, S., Brivio, D., & Grassini, P. (2011). Pemfc system simulation in matlab-simulink® environment. *International Journal of Hydrogen Energy*, *36*, 8045–8052. https://doi.org/10.1016/j.ijhydene.2011.01.093

Rabbani, A., & Rokni, M. (2013). Dynamic performance of a pem fuel cell system. dtu mechanical. *(DCAMM Special Report; No. S154).*

Sharifi Asl, S. M., Rowshanzamir, S., & Eikani, M. H. (2010). Modelling and simulation of the steady-state and dynamic behaviour of a pem fuel cell. https://doi.org/10.1016/j.energy.2009.12.010

Tadbir, M. A., Shahsavari, S., Bahrami, M., & Kjeang, E. (2012). *Thermal management of an air-cooled pem fuel cell: Cell level simulation*.

Wang, C.-Y. (2004). Fundamental models for fuel cell engineering. https://doi.org/10.1021/cr020718s

Wang, L., Husar, A., Zhou, T., & Liu, H. (2003). A parametric study of pem fuel cell performances. *International Journal of Hydrogen Energy*, *28*, 1263–1272. https://doi.org/10.1016/S0360-3199(02)00284-7

Xue, X., Tang, J., Smirnova, A., England, R., & Sammes, N. (2004). System level lumped-parameter dynamic modeling of pem fuel cell. *Journal of Power Sources*, *133*, 188–204. https://doi.org/10.1016/j.jpowsour.2003.12.064

Yang, Z., Du, Q., Jia, Z., Yang, C., Xuan, J., & Jiao, K. (2019). A comprehensive proton exchange membrane fuel cell system model integrating various auxiliary subsystems. *Applied Energy*, *256*, 113959. https://doi.org/10.1016/j.apenergy.2019.113959

Yu, X., Zhou, B., & Sobiesiak, A. (2005). Water and thermal management for ballard pem fuel cell stack. *Journal of Power Sources*, *147*, 184–195. https://doi.org/10.1016/j.jpowsour.2005.01.030

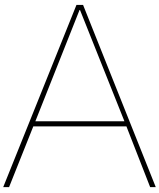

Overview of Simulink submodels

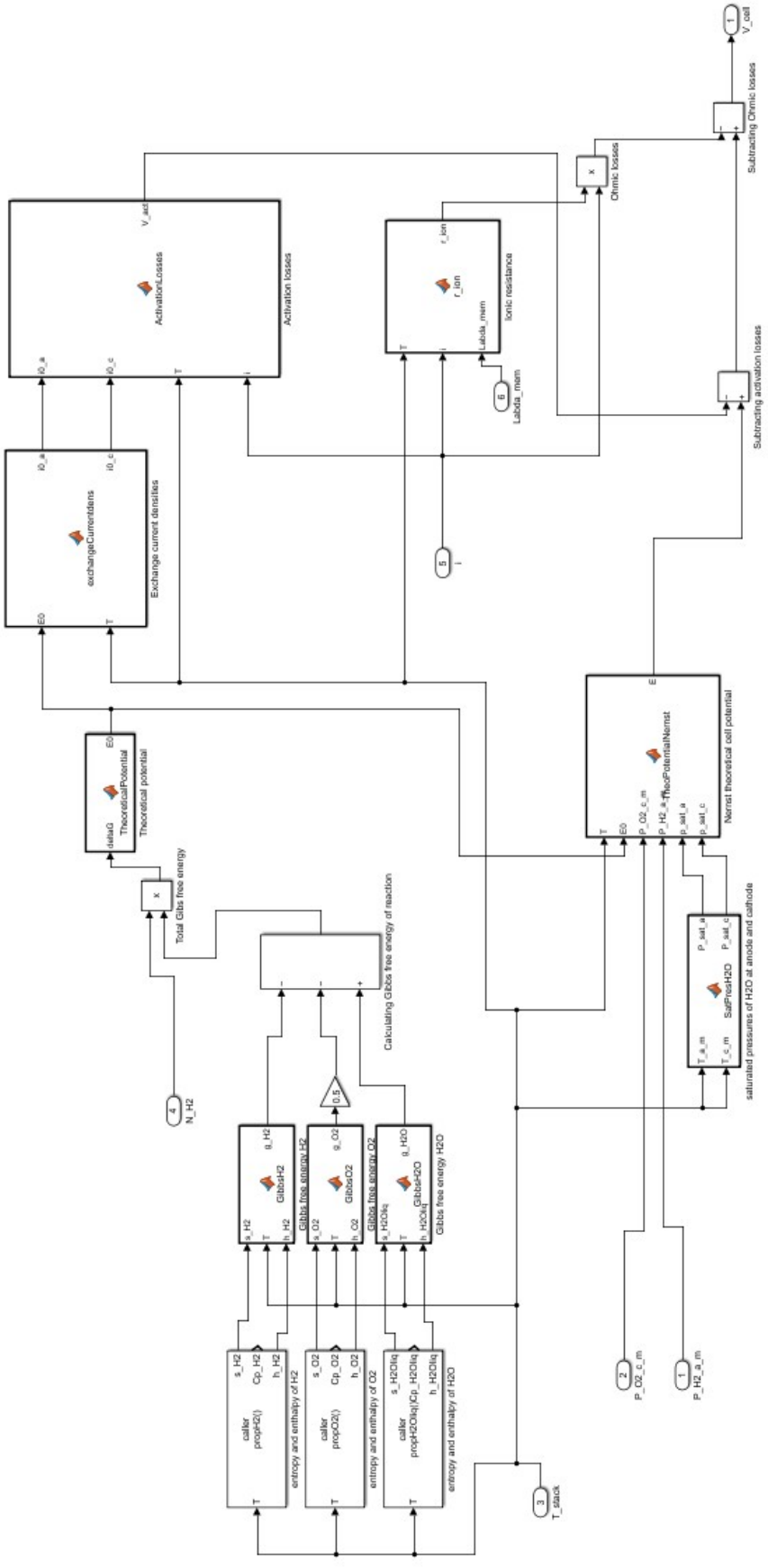

Figure A.1: Implementation of the Electrochemical Balance submodel

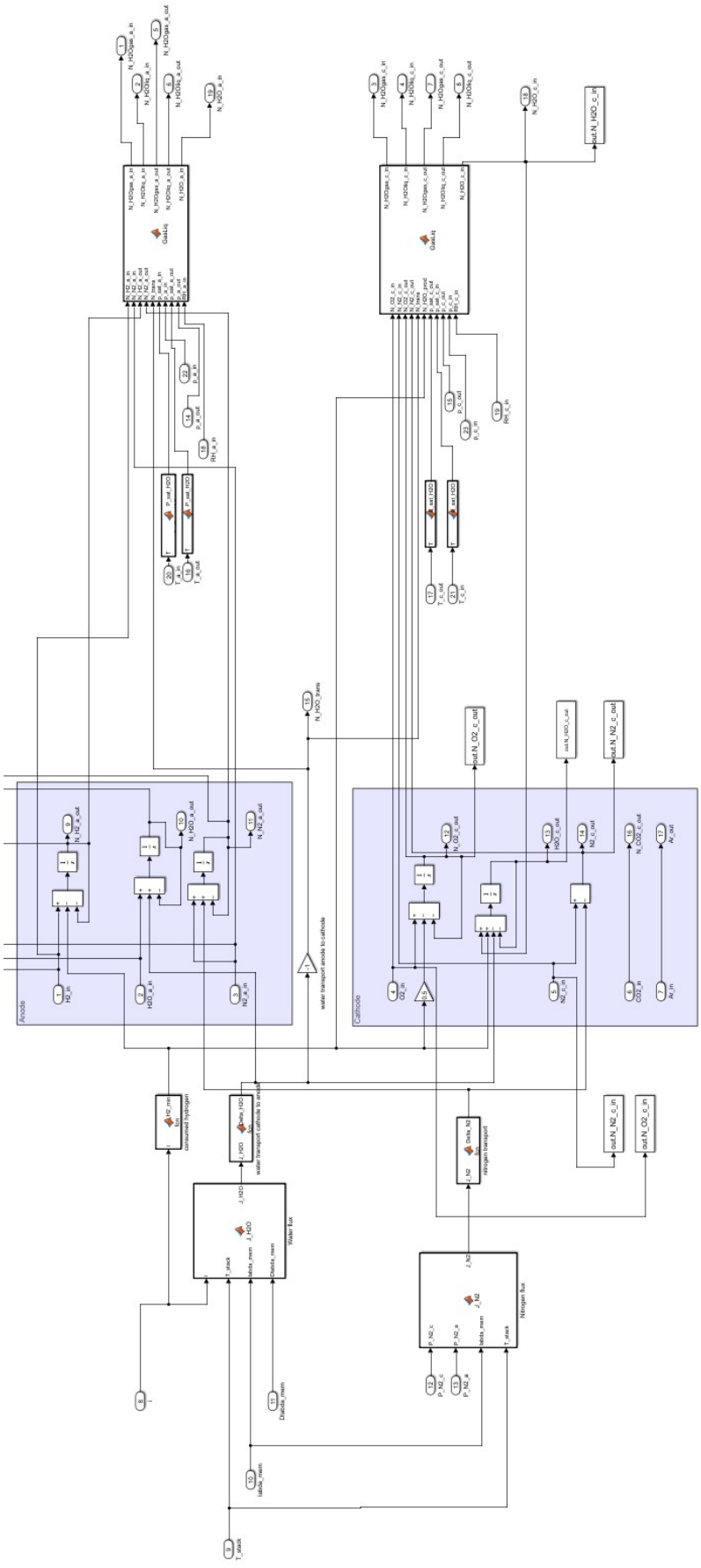

Figure A.2: Implementation of the Molar Flow submodel

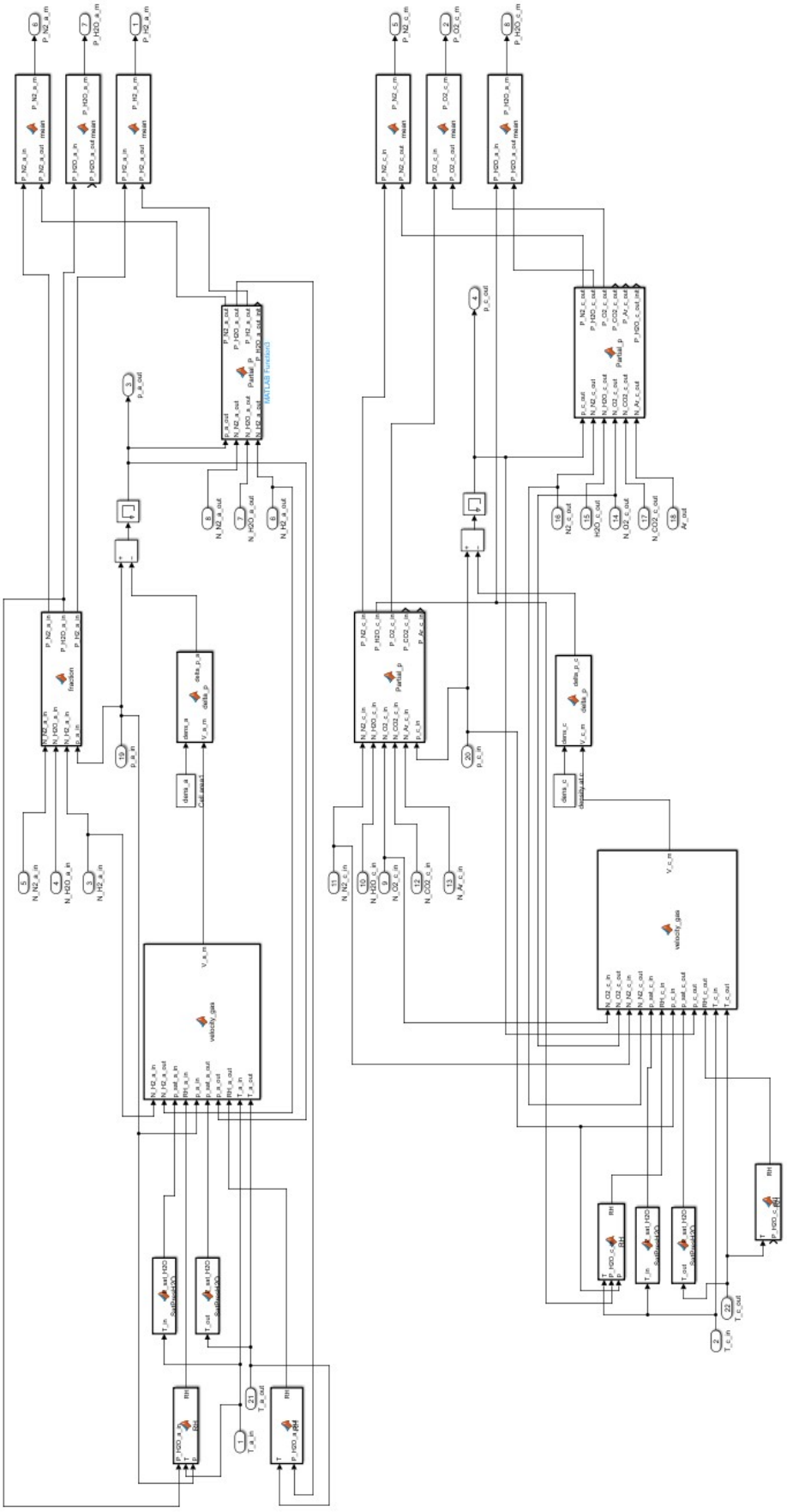

Figure A.3: Implementation of the Pressures and Partial Pressures submodel

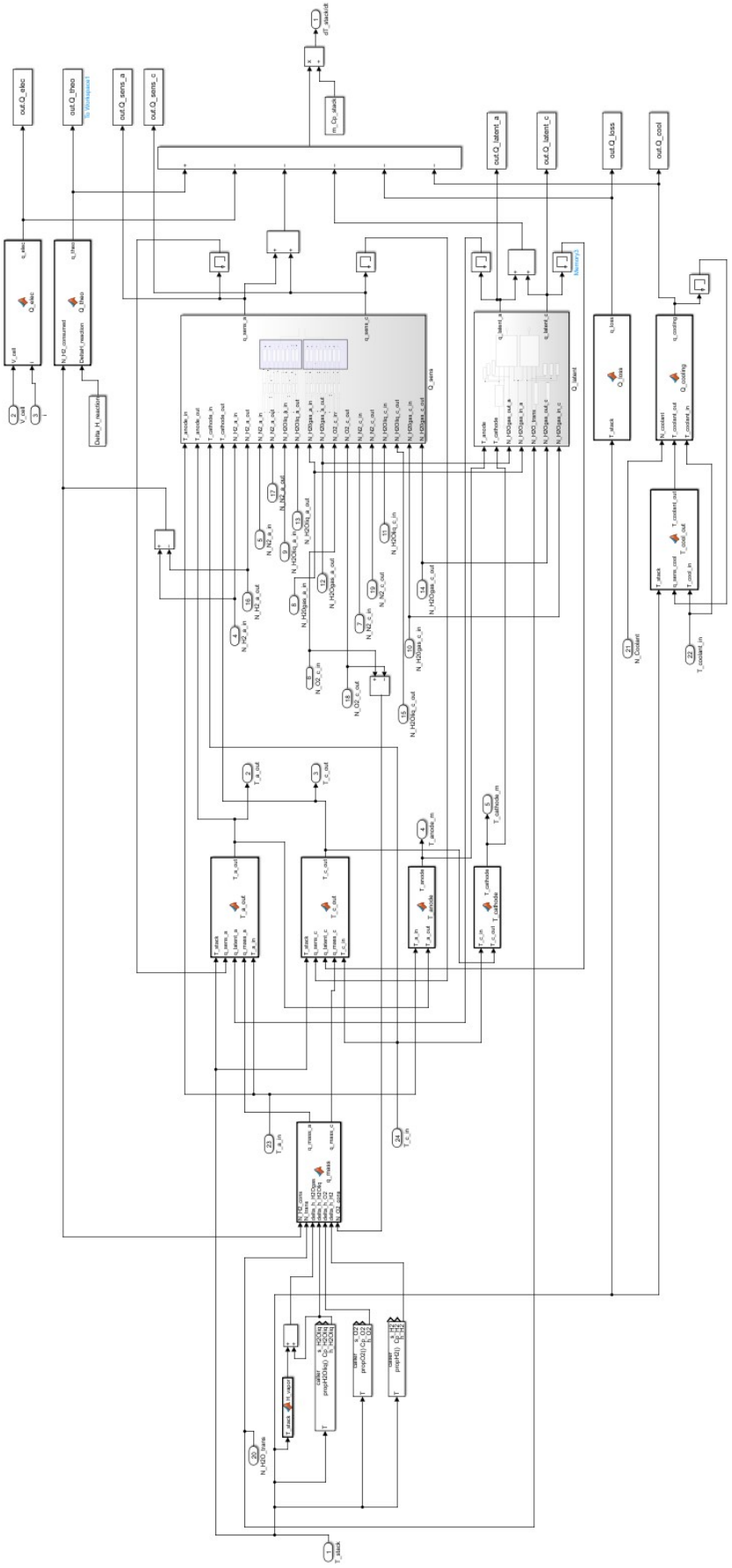

Figure A.4: Implementation of the Energy Balance submodel

B

MatLab script for model parameters

```
disp("Running Set A")
clear;
clc;

%% initial values integrator blocks and memory blocks
init_flowH2_a = 0.000777;
init_flowH2O_a = 0.00005;
init_flowH2O_c = 0.0000001;
init_flowN2_a = 0.0000001;
init_flowO2_c = 0.0000001;
init_P_N2_a_m = 0;
init_P_N2_c_m = 0.1;
init_P_H2O_c_m = 0.015;
init_Pout_a = 1;
init_Pout_c = 1;
init_Qcool = 3;
init_Qlatent_a = 0;
init_Qlatent_c = 1;
init_Qsens_a = 5;
init_Qsens_c = 0;
init_Tstack = 300;

%% test case A I=20A Amphlett et al.
 I = 20; %[A]
 T_setT = 353; %[K]
 A_cell = 232; %[cm^2] area of single fuel cell
 n_cells = 35; %[-] number of cells in stack
 m_Cp_stack = 4600; %[J/K]

stoic_H2 =1.5; %stoichiometric value for the Hydrogen flow
T_a_in = 23.5+273.15; %[K] temperature anode inlet
p_a_in = 1; %[bar] pressure at anode inlet

stoic_air =1.5; %stoichiometric value for the air flow
T_c_in = 23.5+273.15; %[K] temperature cathode inlet
p_c_in = 1; %[bar] pressure at cathode inlet
T_cool_in = 23.5+273.15; %[K] temperature coolant at inlet of stack cooler

 L_a = 0.2; % [m] length of channels on anode side of cell
 D_a = 0.003; % [m] diameter of channels anode
 L_c = 0.2; % [m] length of channels on cathode side of cell
 D_c = 0.003; % [m] diameter of channels cathode
 n_channel = 33; % number of channels in cell

relat_humid_c = 0.8; %[] relative humidity air cathode intake
relat_humid_a = 0.6; %[] relative humidity hydrogen intake dry gas
dens_a = 0.0899; % [kg/m^3]
dens_c = 1.29; % [kg/m^3]

N_N2_a = 0; %molar flow of nitrogen at inlet anode

% parameters overall
R = 8.314; % [J/mol*K] universal gas constant
```

```
F = 96485; % [C/mol] Faraday's constant
p_atm = 1; %[atm] standard atm pressure

% parameters fuel stack
A_fc = A_cell*n_cells; %[cm^2] total area of fuel cells
Delta_H_reaction = 286000; %[J/mol] enthalpy of combustion of hydrogen
hA_a = n_cells*2;%[W/K] heat transfer coefficient* exchange area anode
hA_c = n_cells*10;%[W/K] heat transfer coefficient* exchange area cathode

%membrane parameters
t_m = 0.0183; %[cm] membrane thickness Nafion 117
M_m = 1.1*1000; %[g/mol] molecular weight of membrane Nafion 117
dens_m_dry = 3.28; %[g/cm^3] density of dry membrane Nafion 117
V_w = 18; % [cm^3/mol] molar volume of liquid water dependent on T
V_mem = M_m/dens_m_dry; % [cm^3/mol] molar volume of dry membrame

%electrochemical model
g0_H2O = -237180; %[J/mol] gibbs specific function of formation ...
                                    %at 298K and 1 atm A-25 Moran
T_ref = 25+273.15; %[K] reference temperature Gibbs
s_ref_H2O = 69.95; %[J/(mol*K)] entropy H2O at reference temp and pressure
s_ref_H2 = 130.7; %[J/(mol*K)]
s_ref_O2 = 205.1; %[J/(mol*K)]

i_loss = 0.002; % [A/cm^2] i/nternal current density
beta = 0.5; % [-] symmetry factor
n_elc = 1; % [-] number of electrons in rate step reaction cathode side
n_ela = 4; % [-] number of electrons in rate step reaction anode side
n_H2 = 2; % [-] number of electrons per reaction
k_a = 1; % [mol/(s*cm^2)] ????
k_c = 1; % [mol/(s*cm^2)] ????

n_drag_sat = 2.5; %[-] saturated electro-osmotic drag

%q_loss
R_th = 17; %thermal resistance based on steady-state loss

%pressure calculations
A_channel = pi*(D_a/2)^2; % [m^2] cross-sectional area of channel
mu_a = 1.04*10^(-5); %[Pa*s] absolute viscosity at 100 degrees celsius
mu_c = 2.20*10^(-5); % [Pa*s] absolute viscosity at 100 degrees celsius
capacity_flow =n_cells*(L_c*A_channel*n_channel)/(29/1000); %[mol]

%parameters Cooling circuit
Cp_coolant = 4197.6*0.01802;%[J/mol*K] specific heat coolant
hA_cool = n_cells*50;
%%
disp("Parameters read");
```